



2002

## **A Study of the Three-Dimensional Structure and the Recombinant Expression of Native, Monomeric Vitronectin: An Approach Using Biophysical Chemistry, Immunochemistry, Crystallography, and Molecular Biology**

John C. Fisher, Jr.

Follow this and additional works at: [https://trace.tennessee.edu/utk\\_interstp2](https://trace.tennessee.edu/utk_interstp2)

---

### **Recommended Citation**

Fisher, Jr., John C., "A Study of the Three-Dimensional Structure and the Recombinant Expression of Native, Monomeric Vitronectin: An Approach Using Biophysical Chemistry, Immunochemistry, Crystallography, and Molecular Biology" (2002). *Senior Thesis Projects, 1993-2002*.  
[https://trace.tennessee.edu/utk\\_interstp2/95](https://trace.tennessee.edu/utk_interstp2/95)

This Project is brought to you for free and open access by the College Scholars at TRACE: Tennessee Research and Creative Exchange. It has been accepted for inclusion in Senior Thesis Projects, 1993-2002 by an authorized administrator of TRACE: Tennessee Research and Creative Exchange. For more information, please contact [trace@utk.edu](mailto:trace@utk.edu).

**A STUDY OF THE THREE-DIMENSIONAL STRUCTURE  
AND THE RECOMBINANT EXPRESSION OF NATIVE,  
MONOMERIC VITRONECTIN: AN APPROACH USING  
BIOPHYSICAL CHEMISTRY, IMMUNOCHEMISTRY,  
CRYSTALLOGRAPHY, AND MOLECULAR BIOLOGY**

A Thesis Presented  
to the College Scholars for the  
Bachelors of Science Degree  
The University of Tennessee, Knoxville

John C. Fisher, Jr.



## DEDICATION

This thesis is dedicated to my mother, Vicki Fisher, whose  
loving heart, unbreakable strength, gentle spirit, and beautiful smile  
will forever be my inspiration.



## DEDICATION

This thesis is dedicated to my mother, Vicki Fisher, whose loving heart, unbreakable strength, gentle spirit, and beautiful smile will forever be my inspiration.

Based on investigations into vitronectin-ligand structure/function relationships and threading methods, a computational model of vitronectin's three-dimensional structure was designed organizing vitronectin into several domains including an amino-terminal (N-terminal) somatomedin-B domain, a central hemopexin homology domain, and a C-terminal heparin binding domain. Although our structural model is a compelling foundation to understanding its ligand-binding interactions, we remain cautious and seek to confirm vitronectin's structure empirically.

The purpose of this study is to use techniques in x-ray crystallography to elucidate the three-dimensional structure of full-length, native, monomeric vitronectin and ultimately determine the specifics of the various ligand-binding interactions that confer vitronectin with its dynamic functions. In addition, preliminary work towards a novel recombinant expression system using baby hamster kidney (BHK) cells has been performed using several techniques of molecular biology.



## TABLE OF CONTENTS ABSTRACT

Vitronectin is a multifunctional glycoprotein found in human serum as well as in the extracellular matrix (ECM). Vitronectin is found in circulation as a monomer, both as a double-chain form and a single-chain form, which results from proteolytic cleavage at the carboxy-terminal (C-terminal) position 379. Tissue and matrix associated vitronectin, however, is multimeric. Human vitronectin interacts with a variety of ligands implicated in controlling a number of physiological processes. These biological targets include heparin, plasminogen activator inhibitor-1 (PAI-1), proteases such as thrombin and urokinase-type plasminogen activator (uPA), serine protease inhibitor-protease complexes, the uPA receptor (uPAR), and a sub-class of cell-surface integrin receptors.

Based on investigations into vitronectin-ligand structure/function relationships and threading methods, a computational model of vitronectin's three-dimensional structure was designed organizing vitronectin into several domains including an amino-terminal (N-terminal) somatomedin-B domain, a central hemopexin homology domain, and a C-terminal heparin binding domain. Although our structural model is a compelling foundation to understanding its ligand-binding interactions, we remain cautious and seek to confirm vitronectin's structure empirically.

The purpose of this study is to use techniques in x-ray crystallography to elucidate the three-dimensional structure of full-length, native, monomeric vitronectin and ultimately determine the specifics of the various ligand-binding interactions that confer vitronectin with its dynamic functions. In addition, preliminary work towards a novel recombinant expression system using baby hamster kidney (BHK) cells has been performed using several techniques of molecular biology.



# TABLE OF CONTENTS

| <b>CHAPTER</b>  | <b>Page</b> |
|---|-------------|
| <b>1. VITRONECTIN: AN OVERVIEW OF STRUCTURAL AND FUNCTIONAL PROPERTIES</b>  | <b>1</b>    |
| Introduction  | 1           |
| Localization and Tissue Distribution  | 2           |
| Vitronectin Function  | 4           |
| Structural Organization   | 12          |
| The Signal Sequence   | 15          |
| The Somatomedin B Domain  | 15          |
| The Cell-binding Sequence   | 16          |
| The Connecting Region   | 17          |
| The Hemopexin Repeats   | 18          |
| The Heparin-binding Sequence  | 19          |
| Functional Regulation   | 22          |
| Conformational Lability   | 23          |
| Differential Localization   | 28          |
| Enzymatic Modification  | 30          |
| Computational Model   | 32          |
| <b>2. CRYSTALLIZATION/CO-CRYSTALLIZATION OF FULL-LENGTH, NATIVE, MONOMERIC VITRONECTIN</b>                                | <b>36</b>   |
| <b>3. EXPRESSION OF RECOMBINANT, FULL-LENGTH, NATIVE, MONOMERIC VITRONECTIN IN BABY HAMSTERT KIDNEY CELLS (BHK cells)</b> | <b>64</b>   |
| <b>5. REFERENCES</b>  | <b>70</b>   |



## LIST OF TABLES

### LIST OF FIGURES

#### Table

#### Figure

|     |   |    |
|-----|---|----|
| 1-I | Distribution, Function and Specificities of Vitronectin-Binding Integrin....                          | 10 |
| 1-1 | The Crystal Structure of $\alpha$ Thrombin and Antithrombin III.....                                  | 6  |
| 1-2 | Structure of Active and Latent PAI-1 .....  | 9  |
| 1-3 | Cleavage Sites for Trypsin-like Proteases and Elastase.....   | 13 |
| 1-4 | Binding Functions of Vitronectin Peptides .....   | 14 |
| 1-5 | Encrypted Heparin Binding Site Model .....  | 25 |
| 1-6 | Mechanism of Vitronectin Multimerization .....  | 27 |
| 1-7 | Computational Model of Vitronectin Three-Dimensional Structure .....                                  | 33 |
| 2-1 | One and Two Chain Vitronectin Structural Forms.....   | 41 |
| 2-2 | Protein-Protein Lattice Contacts vs. Non-specific Protein-Protein Contacts ....                       | 42 |
| 2-3 | Numerical Representations for Crystal Screen Condition Scoring.....                                   | 46 |
| 3-1 | Antigen-Fab Crystal Packing.....  | 50 |
| 3-2 | Fab molecules in a crystal lattice and the Unit Cell .....  | 52 |
| 3-3 | Space Filling Model of a Mouse IgG <sub>2a</sub> .....  | 54 |
| 3-4 | Direct ELISA to measure the titer of GMA <sub>500</sub> Anti-Vitronectin Monoclonal<br>Antibody ..... | 58 |
| 4-1 | pUC18 Restriction Map.....  | 67 |
| 4-2 | NotIVNNotI PCR Amplicon .....   | 68 |
| 4-3 | PCR Product Analysis.....   | 69 |



## LIST OF FIGURES

### Figure

|     |  |    |
|-----|--|----|
| 1-1 | The Crystal Structure of $\alpha$ Thrombin and Antithrombin III.....                                 | 6  |
| 1-2 | Structure of Active and Latent PAI-1 .....   | 9  |
| 1-3 | Cleavage Sites for Trypsin-like Proteases and Elastase.....  | 13 |
| 1-4 | Binding Functions of Vitronectin Peptides .....  | 14 |
| 1-5 | Encrypted Heparin Binding Site Model .....   | 25 |
| 1-6 | Mechanism of Vitronectin Multimerization .....   | 27 |
| 1-7 | Computational Model of Vitronectin Three-Dimensional Structure .....                                 | 33 |
| 2-1 | One and Two Chain Vitronectin Structural Forms.....  | 41 |
| 2-2 | Protein-Protein Lattice Contacts vs. Non-specific Protein-Protein Contacts.....                      | 42 |
| 2-3 | Numerical Representations for Crystal Screen Condition Scoring.....                                  | 46 |
| 3-1 | Antigen-Fab Crystal Packing.....   | 50 |
| 3-2 | Fab molecules in a crystal lattice and the Unit Cell.....  | 52 |
| 3-3 | Space Filling Model of a Mouse IgG <sub>2a</sub> .....   | 54 |
| 3-4 | Direct ELISA to measure the titer of GMA <sub>900</sub> Anti-Vitronectin Monoclonal<br>Antibody..... | 58 |
| 4-1 | pUC18 Restriction Map.....   | 67 |
| 4-2 | NotIVNNotI PCR Amplicon.....   | 68 |
| 4-3 | PCR Product Analysis.....  | 69 |



## ABBREVIATIONS USED

|          |   |
|----------|---|
| BSA      | bovine serum albumin                                |
| CNBr     | cyanogen bromide                                    |
| EDTA     | ethylene diamene tetraacetic acid                   |
| GPI      | glycophosphotidylinositol                           |
| HEPES    | 4-(2-hydroxymethyl)-1-piperazineethanesulfonic acid |
| IgG      | immunoglobulin                                      |
| kD       | kilo Dalton   |
| mAB      | monoclonal antibody                                 |
| MWCO     | molecular weight cutoff                             |
| MMP      | matrix metalloproteinases                           |
| MR       | molecular replacement                               |
| mRNA     | messenger ribonucleic acid                          |
| NMR      | nuclear magnetic resonance                          |
| NOEs     | nuclear oven Hauser effects                         |
| PAI-1    | plasminogen activator inhibitor-1                   |
| PBS      | phosphate buffered saline                           |
| PCR      | polymerase chain reaction                           |
| PEG      | polyethylene glycol                                 |
| SDS-PAGE | sodium dodecyl                                      |
| TAT      | thrombin antithrombin complex                       |
| TPA      | tissue-type plasminogen activator                   |
| Tris     | tris hydroxymethyl aminomethane                     |
| uPA      | urokinase-type plasminogen activator                |
| uPAR     | urokinase plasminogen activator receptor            |
| U.V.     | ultraviolet   |



Although found in circulation and the ECM, vitronectin is synthesized in the liver and expressed at low levels in the lungs, kidneys, skin, and brain (Seiffert, *et. al.*, 1991a and 1991b). Vitronectin is present *in vivo* in two conformationally different forms. Circulating vitronectin is primarily in monomeric form at a concentration of 200-400 µg/ml; tissue and matrix vitronectin are found mainly as a multimer (Preissner, *et. al.*, 1985, Barnes, *et. al.*, 1983).

Numerous functions have been ascribed to vitronectin, although the specifics of have yet to be determined on the atomic level for several reasons: (1) its large size and conformational lability; (2) the lack of an adequate expression system has hindered the use of site-directed mutagenic studies; (3) purification of vitronectin from

## VITRONECTIN STRUCTURE AND FUNCTION: AN OVERVIEW

### Introduction

Vitronectin was discovered in 1967 and was identified as a serum spreading factor with a cell-to-cell adhesive role (Holmes, *et. al.*, 1967). Human vitronectin interacts with a variety of ligands implicated in controlling a number of physiological processes including coagulation, fibrinolysis, tumor metastasis, cellular migration, and the humoral immune response (Preissner, *et. al.*, 1991a and 1991b). These macromolecular targets include heparin, plasminogen activator inhibitor-1 (PAI-1), proteases such as thrombin and urokinase-type plasminogen activator (uPA), serine protease inhibitor-protease complexes, the uPA receptor (uPAR), and a sub-class of cell-surface integrin receptors.



Although found in circulation and the ECM, vitronectin is synthesized in the liver and expressed at low levels in the lungs, kidneys, skin, and brain (Seiffert, *et. al.*, 1991a and 1991b). Vitronectin is present *in vivo* in two conformationally different forms. Circulating vitronectin is primarily in monomeric form at a concentration of 200-400  $\mu\text{g/ml}$ ; tissue and matrix vitronectin are found mainly as a multimer (Preissner, *et. al.*, 1985, Barnes, *et. al.*, 1983).

Numerous functions have been ascribed to vitronectin, although the specifics of its structure have yet to be determined on the atomic level for several reasons: (1) its large size and conformational lability; (2) the lack of an adequate expression system has hindered the use of site-directed mutagenic studies; (3) purification of vitronectin from human serum yields both single-chain and double-chain forms, which cannot be adequately separated; 4) extensive post-translational modification leads to a high degree of sample heterogeneity. One characteristic of vitronectin that has indeed been harnessed for the purposes of research is its high propensity to adhere to surfaces. This adherence property has proved very useful for solid phase structure/function research.

### **Localization and Tissue Distribution of Vitronectin**

In circulation, vitronectin has been found in complexes with PAI-1 (Derklerck, *et. al.*, 1988, Mimuro, *et. al.*, 1989, Wiman, *et. al.*, 1988), the terminal complement C5b7 complex (Podack *et. al.*, 1977), and with the thrombin-antithrombin complex (TAT) (Ill, *et. al.*, 1985). Vitronectin has also been found within platelet extracts and is released from platelet  $\alpha$  granules upon thrombin stimulation (Parker, *et. al.*, 1989, Preissner, *et. al.*, 1989). Using immunohistochemical staining, it has been demonstrated that



vitronectin is present in loose connective tissues of skeletal muscle, lung, kidney, and skin (Hayman, *et al.*, 1983). More recently, it has also been found located in the mineralized bone matrix (Seiffert 1996). There is also an age-dependent accumulation of vitronectin within dermal fibers (Dahlback, *et al.*, 1993). Vitronectin most likely localizes to these tissues from circulation.

Vitronectin mRNA is, however, found predominantly in hepatocytes, and most vitronectin is produced within the liver (Seiffert, *et al.*, 1991a). Vitronectin expression in hepatocytes has been shown to be up-regulated by administering endotoxin (Seiffert, *et al.*, 1994). From these studies, there is evidence that the acute inflammatory response may regulate the synthesis of vitronectin.

A vitronectin knockout mouse has been generated using gene displacement (Zheng, *et al.*, 1995). No vitronectin was found in the serum of the knockout (-/-) mice. Studies performed thus far on these knockout mice have shown that vitronectin deficiency has no observable effect on development, survival, or fertility. Recently however, several studies on the vitronectin-deficient mice describe an important regulatory role for vitronectin in thrombogenesis. In one study, an antithrombotic effect of vitronectin was identified at sites of platelet-rich thrombi (Fay, *et al.*, 1999), with the vitronectin knockout forming thrombi faster than the wild-type mouse. Additionally, in another vascular injury model of occlusive thrombus formation, the absence of vitronectin inhibited reocclusion and thus modulated fibrinolysis (Eitzman, *et al.*, 2000). Arterial thrombi in vitronectin-deficient mice are unstable and frequently embolize (Konstantinides, *et al.*, 2001).



Vitronectin is localized to damaged tissue in different pathological conditions: (1) modified vitronectin characterized by advanced glycosylation and a reduced binding affinity for PAI-1, heparin, and cell surface integrin receptors is found localized in the ECM and vasculature of retinæ in diabetic rats (Hammes, *et. al.*, 1996); (2) anti-vitronectin monoclonal antibodies react with atherosclerotic lesion proteins (Sato, *et. al.*, 1990) and rheumatoid arthritic synovia proteins (Rosenblum, *et. al.*, 1996); (3) although not detected in healthy brain tissue, vitronectin immunoreactivity co-localizes with neurofibrillary tangles in the brain of Alzheimer's patients (Akiyama, *et. al.*, 1991, Gladson, *et. al.*, 1991); (4) vitronectin is detected in numerous inflamed and necrotic tissues including the cirrhotic liver (Inuzuka, *et. al.*, 1992), cancerous breast tissue (Niculesca, *et. al.*, 1992), and in areas of acute myocardial infarction (Rus, *et. al.*, 1987).

Target ligands for vitronectin include components of the ECM, cell-surface integrin receptors, participants of the fibrinolytic and coagulatory pathways, and complement factors. Together with the information concerning vitronectin's tissue distribution, these macromolecular targets suggest an important role for vitronectin in wound healing and repair, tissue remodeling, angiogenesis, and tumor metastasis.

### **Vitronectin Function**

As previously mentioned, vitronectin is an important regulatory protein implicated in the control of coagulation, inflammation, and wound healing. The events leading to thrombus formation constitute the dynamic coagulation pathway. When an insult damages a blood vessel wall, a proteolytic cascade induces cleavage of the inactive zymogen prothrombin into its active form, thrombin. The crystal structure of  $\alpha$  thrombin



and antithrombin III is shown in figure 1-1. Thrombin belongs to the serine protease enzyme family, and once activated, it initiates the formation of a thrombus by cleaving another protein, fibrinogen. The products of the fibrinogen cleavage reaction are insoluble fibrin molecules that aggregate to form the proteinaceous meshwork of the thrombus. Thrombin is subsequently inactivated by the serine protease inhibitor (serpin) antithrombin, which binds thrombin in its active site forming an inactive protease inhibitor complex (Rosenberg, *et. al.*, 1973). Proteoglycans, such as heparin, present at blood vessel wall surfaces accelerate the otherwise slow inhibitory activity of antithrombin. The mechanism by which antithrombin activity is accelerated occurs by antithrombin binding the specific pentasaccharide sequence of heparin, inducing a conformational change in antithrombin that enhances the rate at which antithrombin binds thrombin (Olson, *et. al.*, 1981). Moreover, heparin serves as a scaffold on which thrombin and antithrombin interaction can take place, allowing increased local concentrations of both proteins (Peterson, *et. al.*, 1987). Such functions of heparin explain its ability to serve as an anti-coagulant frequently utilized in clinical medicine (Patrick, *et al.*, 1991).

The heparin-vitronectin complex formation has a binding constant in the micromolar range (Zhuang, *et. al.*, 1997). Vitronectin neutralizes the anti-coagulant activity of heparin by competing with both thrombin and antithrombin for heparin binding (Preissner, *et. al.*, 1987). Vitronectin also binds to the inactive TAT (Ill, *et. al.*, 1985). Once vitronectin binds TAT, the inactive complex is hastily cleared from circulation (de Boer, *et. al.*, 1993, Shifman, *et. al.*, 1982).



After an injury, the complement cascade is initiated to prevent infiltration of foreign bacteria. Via proteolytic modification, complement factor C5 is activated to C5b (Muller-Eberhard, *et. al.*, 1966). C5b subsequently reacts with two additional complement proteins, C6 and C7 respectively. The C7 binding event renders the complex amphipathic, allowing it to insert itself within the membrane. Alternatively, the

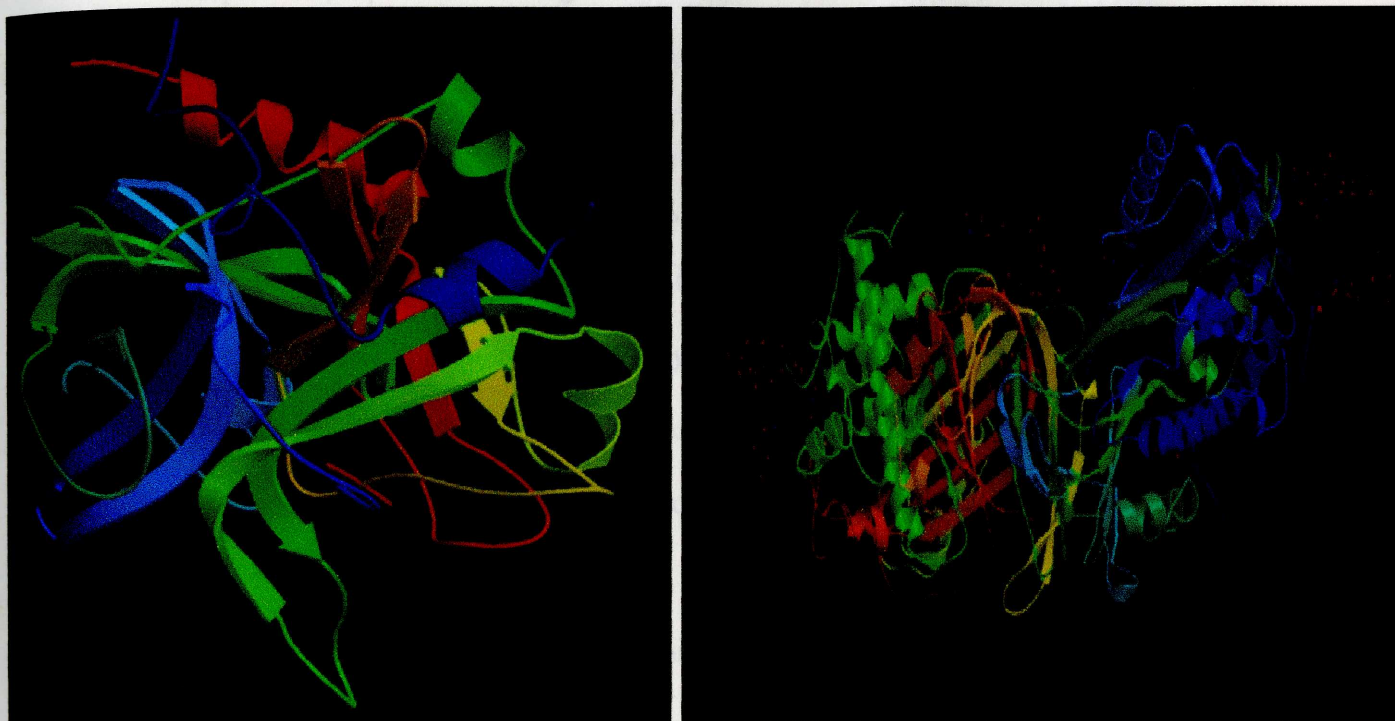


**Figure 1-1:** The crystal structure of  $\alpha$  thrombin (A) and antithrombin III (B).  $\alpha$  thrombin is composed of a 6 kD "A" chain, which is covalently linked to a 31 kD "B" chain through a single disulfide bond. Antithrombin III contains three intra-chain disulfide bonds, a carbohydrate rich domain, an N-terminal heparin binding domain, and a C-terminal serine protease binding domain. The mechanism of TAT complex formation involves the formation of a stable 1:1 complex between the active site of thrombin and the scissile bond (R 385-S 386) of antithrombin III. The active serine of thrombin has been shown to form a covalent intermediate with the P<sub>1</sub> amino acid (R 385) of antithrombin III (Rosenberg, *et. al.*, 1973).

forming an inactive protease-inhibitor complex (Haber, *et. al.*, 1989). It has been deduced from many structure/function studies and from x-ray crystallographic work that PAI-1 exists in two conformationally different forms, an active form and a latent



form After an injury, the complement cascade is initiated to prevent infiltration of foreign bacteria. Via proteolytic modification, complement factor C5 is activated to C5b (Muller-Eberhard, *et. al.*, 1986). C5b subsequently reacts with two additional complement proteins, C6 and C7 respectively. The C7 binding event renders the complex amphipathic, allowing it to insert itself within the membrane. Alternatively, the C5b-7 complex can react with C8 forming the C5b-8 complex responsible for catalyzing polymerization of complement factor C9, in turn generating a membrane-penetrating tubule with cytolytic activity (Tschopp, *et. al.*, 1985). Vitronectin is capable of limiting the lysis of neighboring cells by inhibiting the cytolytic activity of the membrane attack complex (MAC). Vitronectin binds a hydrophobic site on the C5b-7 complex, preventing its insertion into the plasma membrane (Podack, *et. al.*, 1978). Vitronectin also protects against cytotoxic T cell-mediated cell lysis through inhibition of the perforin polymerization (Tschopp, *et. al.*, 1985). *ebb, et. al., 1986). After an insult, multimeric*

matrix At the thrombus, platelets are induced to release proteases by thrombin stimulation, and these proteases commence the wound healing/repair process. This proteolytic enzyme increase is involved in fibrinolysis. Plasminogen activators cleave plasminogen to its active form, plasmin, which subsequently degrades the fibrin meshwork of the clot. PAI-1 is responsible for the inactivation of plasminogen activators, which limits the generation of plasmin (Heckman, *et. al.*, 1988). Like antithrombin, PAI-1 is a serpin, and it binds the active sites of plasminogen activators by forming an inactive protease-inhibitor complex (Huber, *et. al.*, 1989). It has been determined from many structure/function studies and from x-ray crystallographic work that PAI-1 exists in two conformationally different forms, an active form and a latent



form (Fig. 1-2) (Sharp, *et al.*, 1999, Mottonen, *et al.*, 1992, Nar, *et al.*, 2000). The active-to-latent transition of PAI-1 involves incorporation of a surface-exposed loop containing the reactive center into the central  $\beta$ -sheet of the protein. Using site-directed mutagenesis (Lawrence, *et al.*, 1994), monoclonal antibodies (van Meijer, *et al.*, 1994, Wind, *et al.*, 2001), and a combination of peptide mapping and recombinant protein fusions (Padmanabhan, *et al.*, 1995), a vitronectin-binding site on PAI-1 has been localized to residues that lie within the central  $\beta$ -sheet and adjacent secondary structures. Apparently, vitronectin contacts residues in the vicinity of the central  $\beta$ -sheet of PAI-1, thus constraining movement of the strands that is necessary for incorporation of the reactive loop into the central  $\beta$ -sheet (Lawrence, *et al.*, 1994, Wind, *et al.*, 2001). Because vitronectin binds PAI-1, an anti-fibrinolytic protein, and stabilizes its active conformation, it functions as a negative fibrinolytic regulator. Vitronectin binds collagen and is an integral part of the ECM (Gebb, *et al.*, 1886). After an insult, multimeric, matrix vitronectin may localize PAI-1 and plasminogen to the injury site in order to regulate proteolytic events requisite for tissue remodeling.

Matrix vitronectin is also a key component in cell-migration and attachment. Vitronectin is capable of binding two classes of cell-surface receptors. It binds the integrin receptor family at its arginine-glycine-aspartic acid (RGD) integrin epitope sequence (Suzuki, *et al.*, 1984). Table 1-I illustrates the distribution, function, and specificities of vitronectin-binding integrins. Integrins are heterodimeric proteins that recognize the RGD sequence in several adhesive proteins such as fibronectin, fibrinogen, and von Willebrand Factor (Pierschbacher, *et al.*, 1987, Ruoslahti, *et al.*, 1987). Each integrin recognizes specific binding targets, and this ligand specificity is



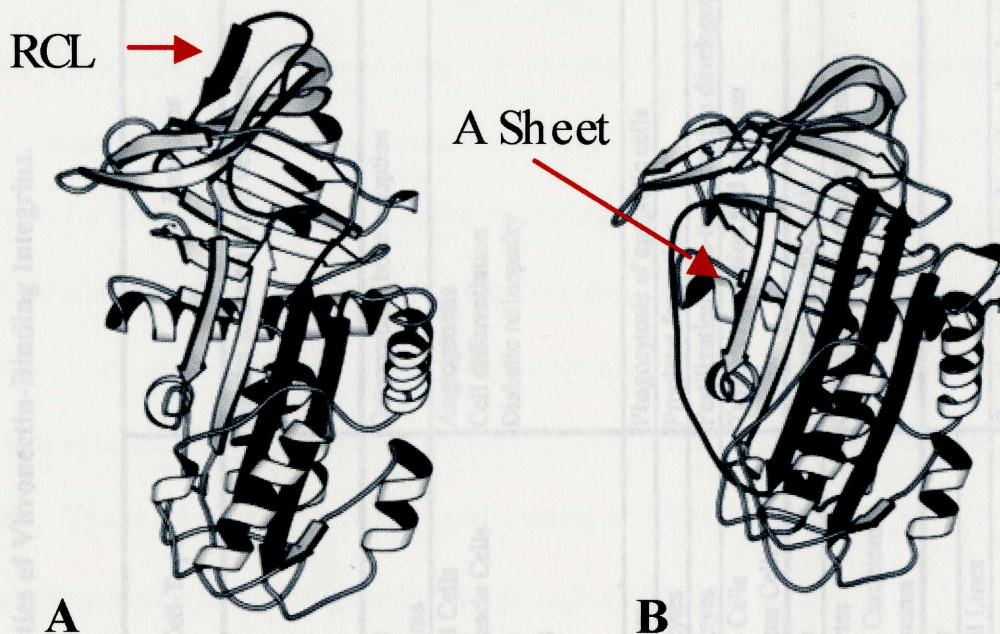


**Figure 1-2 Structure of Active (A) and Latent (B) PAI-1:**

The 3D structure of the active form of PAI-1 (A) illustrates features pertinent to the inhibitory mechanism of proteases by serpins. Serpins are folded around a large, central  $\beta$ -sheet (the A sheet) from which protrudes a surface-exposed loop (the reactive-center loop or RCL). Within this loop region are the residues recognized as substrates by the target protease (uPA or tPA), with the reactive center peptide bond denoted P1-P1'. Upon attack of the protease, this P1-P1' peptide bond of PAI-1 is cleaved by nucleophilic attack of the active-site serine, and an acyl-intermediate is formed. In contrast to the normal progression of proteolysis, this acyl-intermediate is extremely long-lived due to a negligible rate of deacylation. Structural rearrangements occur so that the two ends of the cleaved loop separate, and the P1 end, with the enzyme covalently coupled, is partially inserted into the central  $\beta$ -sheet. As such, the protease is inactivated by formation of a 1:1 stable, covalent complex with the serpin. PAI-1 is unique among the serpins because it readily relaxes from this active form (A) to a latent, inactive form (B). As shown, this occurs by insertion of the RCL into the central  $\beta$ -sheet to contribute a sixth strand to this secondary structural element. This refolding is thermodynamically driven, since the latent form of PAI-1 is more stable.



**Table 1-I: Distribution, Function, and Specificities of Vitronectin-Binding Integrins.**

| <b>Integrin</b>                          | <b>Ligands</b>  | <b>Cell-Type</b>  | <b>Functions</b>   |
|--|---|---|--|
| $\alpha_{IIb}\beta_3$<br>( $II_bIII_a$ ) | Fibrinogen<br>Fibronectin<br>von Willebrand Factor<br>Vitronectin   | Platelets   | Platelet adhesion to the vessel wall                         |
| $\alpha_v\beta_3$                        | Bone Sialoprotein<br>Vitronectin<br>Fibrinogen<br>Fibronectin<br>Perlecan<br>Thrombospondin<br>von Willebrand Factor<br>Vitronectin | Osteoclasts<br>Osteosarcoma   | Osteoporosis, bone resorption                                |
|  |   | Endothelial Cells<br>Smooth Muscle Cells<br>Fibroblasts<br>Leukocytes<br>(others) | Angiogenesis<br>Cell differentiation<br>Diabetic retinopathy |
|  |   | Macrophages   | Phagocytosis of apoptotic cells                              |
|  |   | Megakaryocytes  | Proplatelet formation  |
|  |   | Mouse Oocytes   | Fertilization? Pre-implantation development?                 |
|  |   | Melanoma Cells<br>Glioblastoma Cells  | Tumor progression and invasion                               |
|  |   |   |  |
| $\alpha_v\beta_5$                        | Vitronectin   | Fibroblasts   | Vitronectin endocytosis                                      |
|  |   | Keratinocytes<br>Pancreatic Carcinoma<br>Lung Carcinoma                           | Cell adhesion on vitronectin matrix                          |
| $\alpha_v\beta_1$                        | Vitronectin<br>Fibronectin  | Fibroblasts   |  |
|  |   | Tumor Cell Lines  |  |
|  |   | Mouse Oocytes   | Fertilization? Pre-implantation development?                 |



governed by the particular  $\alpha$  and  $\beta$  subunits of which it is made. Four vitronectin-binding integrins have been identified including  $\alpha_{IIb}\beta_3$ ,  $\alpha_v\beta_3$ ,  $\alpha_v\beta_5$ , and  $\alpha_v\beta_1$  cell-surface receptors (Germer, *et al.*, 1998).  $\alpha_{IIb}\beta_3$  integrin is expressed on platelet surfaces and binds vitronectin, thereby facilitating the adhesion of platelets to the vasculature sub-endothelium during thrombus formation (Thiagarajan, *et al.*, 1988). Within serum, vitronectin functions as the primary cell-spreading factor via its interactions with integrin  $\alpha_v\beta_3$ , which has come to be known as the "vitronectin receptor" (Pytela, *et al.*, 1985 and Horton, *et al.*, 1997). This vitronectin-integrin interaction signals integrin phosphorylation and subsequently endothelial cell differentiation (Bhattacharya, *et al.*, 1995). The  $\alpha_v\beta_5$  receptor mediates endocytosis of ECM-vitronectin by fibroblasts. In fact, vitronectin is the only ligand known for  $\alpha_v\beta_5$  (Panetti, *et al.*, 1993).

Vitronectin binds the urokinase plasminogen activator receptors (uPAR) on monocytes, endothelial cells, and myeloid cells. Binding uPAR promotes the adhesion of these cells to the ECM. Cell migration and ECM degradation is facilitated by protease activity localized to the cell surface. This protease localization is promoted by the binding event between uPAR and urokinase type plasminogen activator (uPA) (Vassali, *et al.*, 1985). uPAR is anchored in the membrane by a GPI moiety (Ploug, *et al.*, 1991), thus intracellular signaling must be transduced via coupling to another receptor. Such coupled linking events are believed to be mediated by integrins. It has been shown that vitronectin binds uPAR at a site different from that of uPA. Moreover, it has been proposed that uPA might have a synergistic effect on the vitronectin binding event (Walt, *et al.*, 1994 and Wei, *et al.*, 1994). PAI-1 and uPAR share a vitronectin binding site, and



PAI-1 competes with uPAR for vitronectin binding subsequently leading to cell detachment and migration (Waltz, *et al.*, 1997; Kjoller, *et al.*, 1997; Deng, *et al.*, 1996).

## Structural Organization

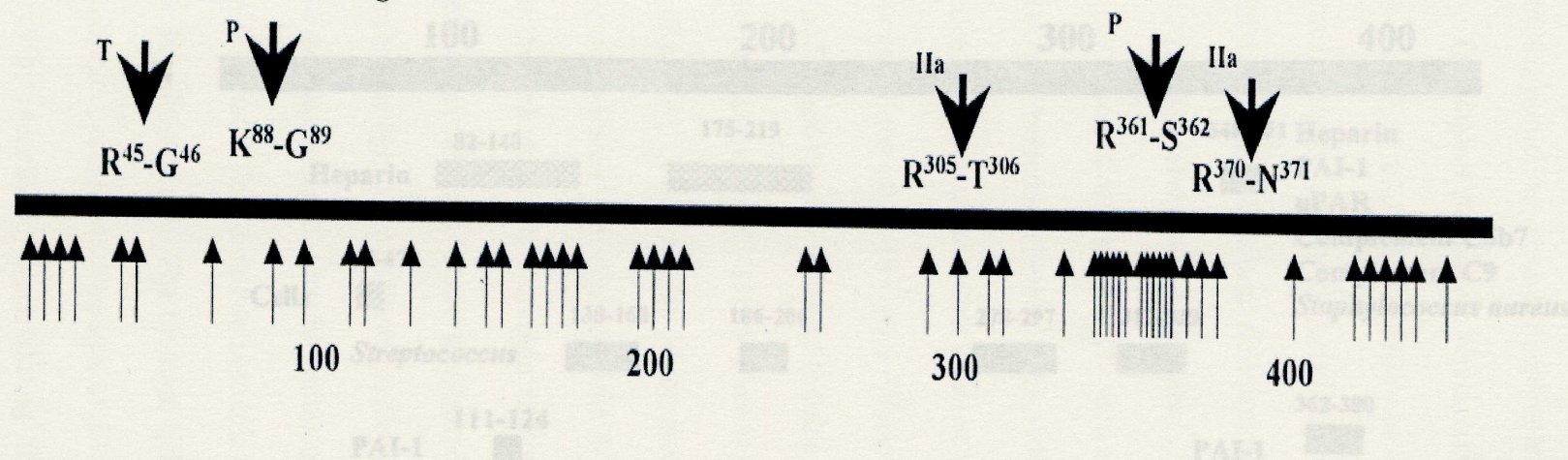
Multi-functional proteins are commonly found to be composed of independently folded domains arranged linearly with respect to amino acid sequence. This means of organization allocates ligand binding to different, independent epitopes. Vitronectin is thought to be such a multi-domain protein.

The multi-domain hypothesis for vitronectin has been supported by proteolytic experiments, because liberated vitronectin fragments often retain their ligand binding function, a fact often indicative of a multi-domain arrangement. There are two sites in vitronectin that are quite accessible to proteolysis: 1) an N-terminal sequence within residues 44 and 90, and 2) a C-terminal site within residues 340-370. Plasmin (Chain, *et al.*, 1991; Gechtman, *et al.*, 1997), thrombin (Gechtman, *et al.*, 1997), and mast-cell tryptase (Cynthia Peterson and David Johnson, unpublished observation) cleave vitronectin within residues 340-370. Prolonged digestion of vitronectin with plasmin and mast-cell tryptase results in N-terminal cleavage between K<sup>88</sup> and G<sup>89</sup> (Kost, *et al.*, 1996). Trypsin cleaves the R<sup>44</sup>-G<sup>45</sup> peptide bond (Sigurdardottir, *et al.*, 1994). An illustrated list of plasmin/trypsin cleavage sites is depicted in figure 1-3.

Synthetic peptides and monoclonal antibodies have also been useful in assigning functional domains to the vitronectin sequence. A number of synthetic peptides have been observed to either mimic vitronectin function or inhibit ligand binding. The binding functions of the various vitronectin peptides are shown in figure 1-4. The use of



### A. Plasmin/Trypsin Cleavage Sites.



### B. Elastase Cleavage Sites.

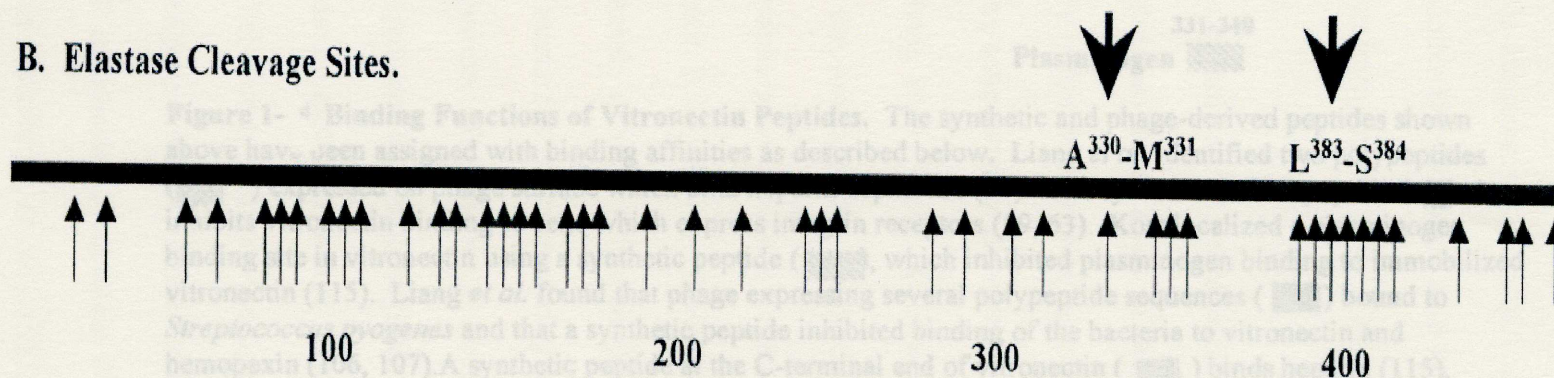
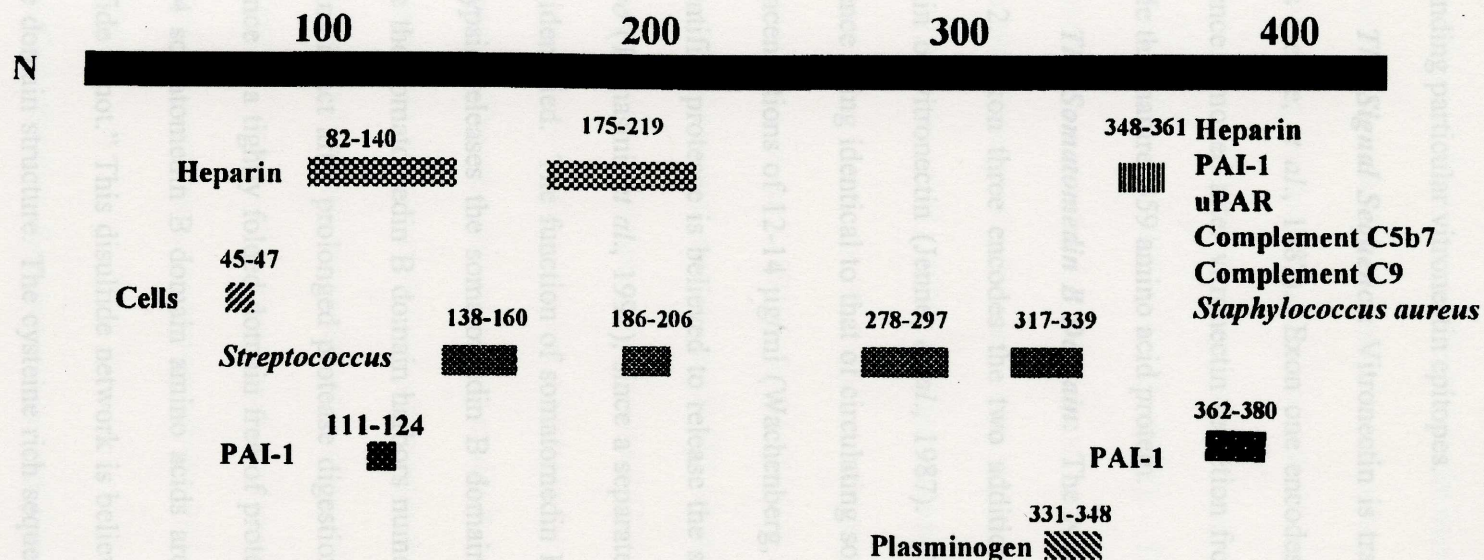


Figure 1-4 Binding Functions of Vitronectin Peptides. The synthetic and phage-derived peptides shown above have been assigned with binding affinities as described below. Lin et al. (115) identified several peptides that bind to vitronectin (115). Lin et al. found that phage expressing several polypeptide sequences (115) which inhibited plasminogen binding to vitronectin (115). A synthetic peptide (115) which inhibited plasminogen binding to vitronectin (115) binds heparin (115), competes with immobilized vitronectin for binding PAI-1 (115), inhibits complement mediated cell lysis by interacting with complement C5b7 (51) and or C9 (120) and mediates binding of vitronectin to *Pseudomonas aeruginosa* (124). A synthetic peptide derived from a sequence close to the N-terminus of vitronectin spans residues 111-124 (115). This peptide stabilizes PAI-1 activity (99). Synthetic peptides corresponding to residues 362-380 also display PAI-1 binding activity (115, 119) (115).





**Figure 1- 4 Binding Functions of Vitronectin Peptides.** The synthetic and phage-derived peptides shown above have been assigned with binding affinities as described below. Liang *et al.* identified two polypeptides ( ) expressed on phage surface which bind heparin-sepharose (98). The synthetic RGDS peptide ( ) inhibits vitronectin binding to cells which express integrin receptors (59, 63). Kost localized a plasminogen binding site in vitronectin using a synthetic peptide ( ), which inhibited plasminogen binding to immobilized vitronectin (115). Liang *et al.* found that phage expressing several polypeptide sequences ( ) bound to *Streptococcus pyogenes* and that a synthetic peptide inhibited binding of the bacteria to vitronectin and hemopexin (106, 107). A synthetic peptide at the C-terminal end of vitronectin ( ) binds heparin (115), competes with immobilized vitronectin for binding PAI-1 (115), inhibits complement mediated cell lysis by interacting with complement C5b7 (51) and or C9 (120) and mediates binding of vitronectin to *Pneumocystis carinii* (124). A synthetic peptide derived from a sequence close to the N-terminus of vitronectin spans residues 111-124 ( ). This peptide stabilizes PAI-1 activity (99). Synthetic peptides corresponding to residues 362-380 also display PAI-1 binding activity (115, 119) ( ).



monoclonal antibodies is based on the ability of some of them to compete with ligands for binding particular vitronectin epitopes.

**The Signal Sequence:** Vitronectin is translated from mRNA assembled from 8 exons (Jenne, *et al.*, 1987). Exon one encodes the 19 amino acid hydrophobic signal sequence removed after vitronectin secretion from hepatocytes. The 7 remaining exons encode the mature, 459 amino acid protein.

**The Somatomedin B Domain:** The N-terminal 42 amino acids are encoded by exon 2. Exon three encodes the two additional amino acids of the somatomedin B domain of vitronectin (Jenne, *et al.*, 1987). This domain was given its name due its sequence being identical to that of circulating somatomedin B, which is present in serum at concentrations of 12-14  $\mu\text{g/ml}$  (Wachenberg, *et al.*, 1980). Cleavage by an as of yet unidentified protease is believed to release the somatomedin B domain from vitronectin *in vivo* (Tomasini, *et al.*, 1991), since a separate gene encoding somatomedin B has not been identified. The function of somatomedin B is unknown. Proteolysis of vitronectin by trypsin releases the somatomedin B domain *in vitro* (Sigurdardottir, *et al.*, 1994). While the somatomedin B domain harbors numerous arginines and lysines, its sequence remains intact after prolonged protease digestion. This ability to resist cleavage offers evidence of a tightly folded domain free of protease accessible regions. In fact, eight of the 44 somatomedin B domain amino acids are cysteines, which form an intradomain disulfide "knot." This disulfide network is believed to facilitate the tightly folded nature of the domain structure. The cysteine rich sequence within vitronectin is homologous to hydrophobic cysteine-rich repeats of B-cell membrane glycoprotein PC-1 (Buckley, *et al.*, 1990), megakaryocyte-stimulating factor (Merberg, *et al.*, 1993), and autotaxin



(Seiffert, *et al.*, 1991). These proteins, however, share no functional similarity to vitronectin or to the somatomedin B domain itself.

Studies including proteolysis and epitope mapping support the localization of a PAI-1 binding site to the somatomedin B domain. It has been demonstrated that PAI-1 could bind a 6-kD CNBr fragment derived from vitronectin's N-terminus, whereas heparin could not (Seiffert, *et al.*, 1991). The cleaved fragment competed against immobilized vitronectin for PAI-1, and only bound PAI-1 in its active conformation. Thrombin cleavage of vitronectin also yields a 38-kD N-terminal fragment that binds PAI-1 (Seiffert, *et al.*, 1991). After cleavage by trypsin, an N-terminal vitronectin fragment was found to bind and subsequently stabilize PAI-1 in its active form (Sigurdardottir, *et al.*, 1994). In addition, a monoclonal antibody that recognizes a vitronectin N-terminal epitope, mAB 153, competed with PAI-1 for vitronectin binding and was capable of disrupting vitronectin-PAI-1 complexes (Seiffert, *et al.*, 1994).

A uPAR binding site has also been localized to the somatomedin B domain of vitronectin. The recombinant somatomedin B domain polypeptide consisting of residues 1-41 competes with immobilized vitronectin for binding the urokinase receptor, and a somatomedin B mutant incapable of binding PAI-1 was unable to bind uPAR (Deng, *et al.*, 1996). mAB 153, mentioned previously, prevents vitronectin from binding immobilized complexes containing uPAR, PAI-1, and plasminogen activator (Deng, *et al.*, 1996).

**Cell Binding Sequence:** An arginine-glycine-aspartic acid (RGD) sequence flanks the somatomedin B domain. This RGD sequence is found to be conserved in a number of ECM proteins including fibronectin, fibrinogen, and von Willebrand Factor. It



has been demonstrated that synthetic peptides derived from the amino acid sequence adjacent to the RGD sequence prevent integrin-bearing cell adhesion to vitronectin (Pierschbacher, *et al.*, 1987; Hayman, *et al.*, 1985). The RGD motif is the primary determinant in integrin-mediated cell binding, as determined by site-directed mutagenesis. Integrin-mediated cell binding activity can be demolished by conservative mutations of the RGD sequence including KGD, RAD, or RGE (Sane, *et al.*, 1993; Cherny, *et al.*, 1993).

**The Connecting Region:** The integrin-binding region connects the somatomedin B domain to a stretch of cysteine-free amino acids (46-130) in vitronectin. It is within this "connecting region" that a number of post-translational modifications are made. Tyrosines 56 and 59 are modified by sulfation (Jenne, *et al.*, 1989). An N-linked glycosylation site is found on asparagine-67 (Tomasini, *et al.*, 1991). Vitronectin is a substrate for transglutaminase and factor XIIIa *in vitro* (Sane, *et al.*, 1993). Transglutamination induces the formation of higher order vitronectin complexes resistant to dissociation by SDS and reducing agents. Glutamine residues 73, 84, 86, and 93 are believed to be the primary transaminoglutaminase substrates in transaminoglutamate reactions due to their incorporation of putrescine after treatment (Skorstengaard, *et al.*, 1990). It has not been established whether transaminoglutaminase-mediated multimerization of vitronectin occurs *in vivo*.

The connecting region harbors binding sites for several ligands. Monoclonal antibodies with connecting region epitopes compete with collagen for binding immobilized vitronectin (Morris, *et al.*, 1994). A polypeptide sequence from within the connecting region binds heparin and is capable of competing for immobilized vitronectin



for heparin binding, as shown by phage display (Liang, *et al.*, 1997). An additional PAI-1 binding site has been localized to the connecting region by screening fragments produced from *Staphylococcus* V8 protease for the ability to bind and subsequently stabilize active PAI-1 (Mimuro, *et al.*, 1993). A vitronectin fragment composed of residues 115-121 has been shown to compete with PAI-1 for binding to immobilized vitronectin. This fragment's ability to stabilize active PAI-1 has also been verified using kinetic assays.

**Hemopexin Repeats:** Two additional homologous domains, residues 131-268 and 269-549, comprise the remainder of the vitronectin sequence. Six cysteines reside within this N-terminal portion. Two of these cysteines are reduced and buried within the molecule's folded structure (Zhuang, *et al.*, 1996). There are two additional N-linked glycosylation sites, asparagines 150 and 223 (Tomasini, *et al.*, 1991). As is found to be characteristic of both the somatomedin B domain and the connecting region, the hemopexin repeats are highly resistant to proteolytic cleavage. The domains have been named for their homology to the symmetrical heme transport protein, hemopexin (Jenne, *et al.*, 1987; Stanley, 1986). The individual domains of hemopexin are composed of 4 tandem repeats. The two domains are connected by a flexible hinge region holding the two domains within close proximity of each other. It is believed that upon binding heme, a conformational change is mediated within the protein, exposing liver cell receptor binding sites at the interface of the two domains (Smith, *et al.*, 1988). Hemopexin-like domains are found in matrix metalloproteinases (MMP) such as collagenase and gelatinase (Wallon, *et al.*, 1997). In these examples, the hemopexin



domains are believed to mediate binding to the ECM, heparin, and cells (Wallon *et al.*, 1997; 103).

Unlike hemopexin, vitronectin has not been found to bind heme, thus the function of the hemopexin tandem repeats of vitronectin has yet to be appreciated. One possibility is that these domains may facilitate binding bacteria. For example, it has been shown that vitronectin exhibits affinity for *Escherichia coli* and might facilitate their adherence to endothelial cells (Valentin-Weigand, *et al.*, 1988). It has also been shown that mannose and various oligosaccharides are capable of inhibiting the binding of vitronectin to *Staphylococcus aureus*, and sialic acid-binding proteins can inhibit vitronectin binding to *Helicobacter pylori*. Such inhibitory data suggests an involvement of sugars in the recognition of bacterial surface proteins (Wadstrom, *et al.*, 1993). Because the hemopexin repeats harbor two of vitronectin's three oligosaccharides, this domain may be a potential bacteria binding target. In fact, peptides from the hemopexin sequence have been shown to have affinity for *Streptococcus pyogenes*. The bacteria bind hemopexin as well as vitronectin, and the binding sequence identified was used to derive synthetic peptides which inhibited the ability of streptococci to bind both hemopexin and vitronectin.

**The Heparin Binding Sequence:** The first hemopexin domain in the vitronectin sequence is complete in the sense that it contains all four tandem repeats found natively in the domains of hemopexin. The second hemopexin domain, however, contains only three hemopexin sequence repeats. Between the second and third tandem repeat of the second hemopexin domain lies a sequence, residues 345-379, of highly charged amino acids. This sequence region harbors two motifs of charged/uncharged amino acids that



corresponds to the heparin-binding consensus sequence derived from numerous heparin-binding proteins (Cardin, *et al.*, 1989; Sobel, *et al.*, 1992). In addition, serine at position 378 is phosphorylated *in vivo*, and it has been found that it can be phosphorylated *in vitro* by protein kinase A (McGuire, *et al.*, 1988; Gechtman, *et al.*, 1997; Korc-Grodzicki, *et al.*, 1998; Korc-Grodzicki, *et al.*, 1990). As previously mentioned, vitronectin circulates in both a two chain form and a one chain form that results from proteolytic cleavage between arginine 379 and alanine 380 (Dahlback, *et al.*, 1985). Unlike the majority of the tightly folded vitronectin sequences, the charged heparin-binding sequence and the sequences flanking either side exhibit increased susceptibility to proteolytic cleavage *in vitro*.

Support for assigning heparin-binding activity to this site in vitronectin is supported by the high degree of similarity it has with other known heparin-binding motifs in proteins such as thrombin, antithrombin, and glial-derived nexin. A number of experimental observations support the assignment as well: 1) a CNBr cleavage product containing the sequence exhibits affinity for heparin in ligand blotting assays, competes for full-length vitronectin for heparin binding, and neutralizes heparin anti-coagulant activity (Suzuki, *et al.*, 1984); and 2) synthetic peptides and monoclonal antibodies with epitopes within this region prevent heparin from binding this sequence on vitronectin (Kost, *et al.*, 1992); 3) plasmin proteolysis within this region has been found to hinder the heparin-binding activity of vitronectin (Gechtman, *et al.*, 1997; Kost, *et al.*, 1996); and 4) removal of sequences 306-370 and 331-383 using thrombin and elastase disrupts the heparin-binding activity of vitronectin (Gechtman, *et al.*, 1997).



**Function:** The heparin binding site serves as a binding site for a number of additional vitronectin target ligands including an additional PAI-1 binding site (Chain, *et al.*, 1991; Preissner, *et al.*, 1990; Sane, *et al.*, 1991; Gechtman, *et al.*, 1993), plasminogen (Preissner, *et al.*, 1990), the complement complex (Tschoppi, *et al.*, 1985; Milis *et al.*, 1993), uPAR (Deng, *et al.*, 1996), and collagen (Ishikawa-Sakurai, *et al.*, 1993; Ishikawa *et al.*, 1992). Evidence supporting uPAR and complement complex binding to the vitronectin heparin-binding sequence stems from studies performed in which a CNBr derived fragment containing the heparin-binding sequence or synthetic peptides derived from the heparin-binding sequence inhibits the binding of these ligands to full-length vitronectin. Localization of a PAI-1 and plasminogen binding sites are better empirically supported.

**Function:** Plasmin cleavage of vitronectin yields a fragment, residues 1-361, that retains the capability to bind plasminogen, suggesting that this cleaved fragment retains a high degree of its natively folded structure (Gechtman, *et al.*, 1997; Kost, *et al.*, 1992). The plasminogen epitope was localized to the C-terminus, for upon treatment of the fragment with carboxypeptidase, the plasminogen-binding activity is disrupted. Using overlapping synthetic peptides derived from the heparin binding site, the plasminogen binding site has been mapped to residues 340-348 (Kost, *et al.*, 1992). Additionally, cathepsin D and *Staphylococcus* V8 protease generated vitronectin fragments have been shown to bind both heparin and plasminogen in ligand-blotting assays (Preissner, *et al.*, 1990).



## Functional Regulation

There are discrepancies regarding the precise assignment of ligand binding sites to vitronectin, nonetheless, our lab follows the general acceptance that ligand binding sites are localized to linear epitopes, which fold into discrete domains. Such binding site organization is capable of accommodating multiple ligands, and it is possible that vitronectin can interact simultaneously with different ligands so as to facilitate a "cross-talk" between separate physiological systems. Some examples found in literature that support this idea include: 1) vitronectin binds glycosaminoglycans concurrently with the TAT complex (de Boer, *et al.*, 1992). The apparent affinity of vitronectin for glycosaminoglycans increases due to interactions during TAT binding (Patrick, *et al.*, 1991). The vitronectin-protease ternary complex is endocytosed by endothelial cells in a manner dependent on the glycosaminoglycan binding site of vitronectin. Such dependence suggests that both TAT and glycosaminoglycan binding functions are essential for vitronectin-mediated protein-inhibitor complex clearance from circulation. 2) Vitronectin is incorporated into the ECM via interactions with collagen and heparin sulfate glycosaminoglycans (Ishikawa, *et al.*, 1992; Sane, *et al.*, 1990; Thiagarajan, *et al.*, 1996). ECM vitronectin binds uPAR and integrin receptors on cells. It also binds plasminogen and PAI-1 (Preissner, *et al.*, 1990; Mimuro, *et al.*, 1987; Owensby *et al.*, 1991). Vitronectin functions as a biological adhesive by interacting with immobilized matrix molecules and cells/plasma molecules, and thus facilitates cellular adherence and localization of fibrinolytic proteins to the endothelium. 3) Vitronectin incorporated into the terminal complement complex stimulates tyrosine phosphorylation in fibroblast cells in an integrin-dependent manner (Bhattacharya, *et al.*, 1995). The RGD and complement



sites on vitronectin function in tandem to convey extracellular inflammatory information to intracellular signal transduction pathways. Vitronectin's domain organization allows it to exhibit multiple functions. The expression of vitronectin function *in vivo* may also be regulated by the protein's oligomeric state, enzymatic modifications, and by its vascular localization.

**Conformational Lability:** Vitronectin is conformationally labile and displays differential binding activities, which depend on the specificity of its fold. It was noted that urea-treated vitronectin was able to bind heparin-Sepharose with greater affinity than non-denatured vitronectin at physiological ionic strength (Barnes, *et al.*, 1985; Hayashi, *et al.*, 1985). This observation led to the speculation of an encrypted heparin-binding sequence in the native fold of the molecule (Hayashi, *et al.*, 1985; Preissner, *et al.*, 1987). For example, heat or pH could mimic the change in fold, resulting in a vitronectin conformer capable of binding heparin more efficiently in solid phase assays. Based on these observations as well as on the sequence homology with hemopexin, it was suggested by Preissner, *et al.* that the cationic heparin-binding sequence was non-functional in native vitronectin due to acidic residue interactions near vitronectin's N-terminus (Preissner, *et al.*, 1987). According to this model, vitronectin adopts an "open" conformation following denaturation exposing the natively encrypted heparin-binding domain. This theory has been widely accepted, and virtually all empirical data is interpreted with the presupposition of an encrypted heparin-binding site.

It has been demonstrated that the monoclonal antibody 8E6, which blocks heparin binding to vitronectin, preferentially recognizes the denatured/renatured form of vitronectin (Tomasini, *et al.*, 1989; Tomasini, *et al.*, 1988). With the contention that the



8E6 epitope was the heparin binding site, this data seemed to support Preissner's encrypted-binding site model. Figure 1-5 illustrates the encrypted heparin binding site model. Moreover, renatured vitronectin binds more avidly to PAI-1 (Lawrence, *et al.*, 1997) and collagen (Ishikawa, *et al.*, 1992) in solid phase assays. Additionally, a CNBr-derived C-terminal fragment of vitronectin prevents complement-mediated cytolysis and inhibits heparin activity more effectively than intact vitronectin (Tschopp, *et al.*, 1988). According to the prevailing encrypted heparin binding site theory, liberating this fragment from the native fold of the molecule increases its accessibility and increases its activity.

Importantly, evidence has recently been found that argues against the encrypted heparin binding site that other functional regions of vitronectin are buried in the native fold of the molecule and increase in activity after refolding. Dietmar Seiffert found that the 8E6 monoclonal antibody, which had been used extensively in support of the encrypted heparin binding site theory, mapped to a sequence within the first hemopexin repeat rather than to the heparin binding site (Seiffert, *et al.*, 1995). Furthermore, other monoclonal antibodies possessing epitopes outside of the heparin binding sequence preferentially recognize refolded vitronectin (Seiffert, *et al.*, 1991). Binding sites for ligands such as PAI-1 and collagen, which display higher affinity for refolded vitronectin, have also been mapped outside of the heparin-binding region of the protein. Integrins, which recognize the N-terminal RGD motif, bind more efficiently to refolded vitronectin (Seiffert, *et al.*, 1997). In accordance with the commonly accepted theory that vitronectin natively adopts a "closed" conformation, most believe that these monoclonal antibodies



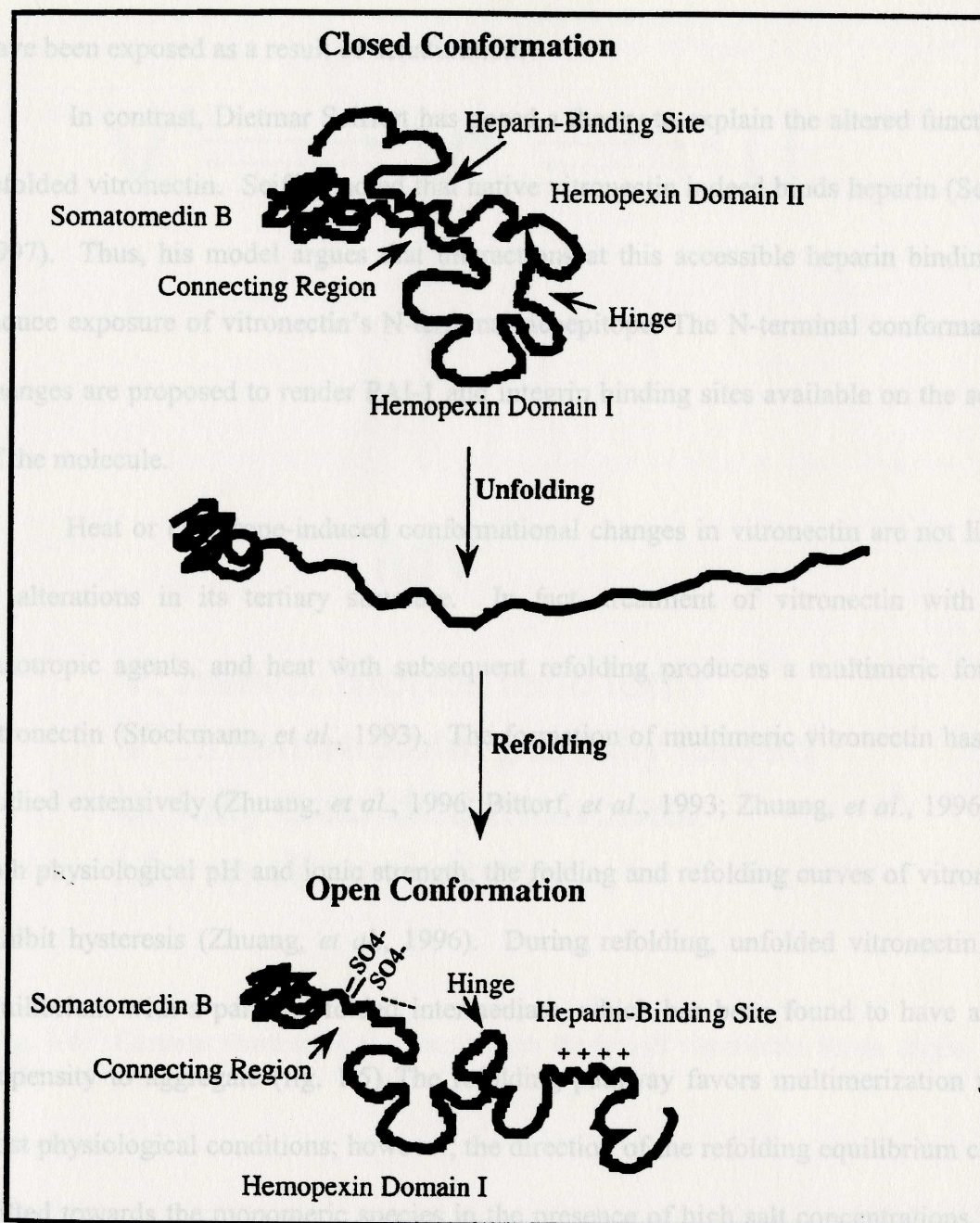


**Fig. 1.5: Encrypted Heparin Binding Site Model.** The model suggested by Preissner *et al* suggests that plasma vitronectin exists in a “closed conformation” stabilized by salt bridges between the cationic heparin binding site and negatively charged sulfated amino acids in the Connecting region. After unfolding and refolding or treatment with certain ligands, the “hinge” region moves the two hemopexin domains apart, exposing the heparin binding site.



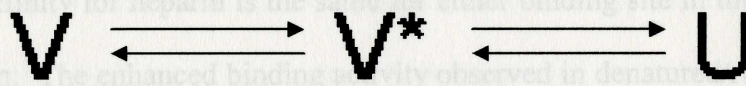
and ligands display enhanced affinity for renatured vitronectin because their binding sites have been exposed as a result of denaturation.

In contrast, Dietmar Seiffert has posed a theory to explain the altered function of refolded vitronectin. Seiffert noted that native vitronectin indeed binds heparin (Seiffert, 1997). Thus, his model argues that interactions at this accessible heparin binding site induce exposure of vitronectin's N-terminal neoepitope. The N-terminal conformational changes are proposed to render PAI-1 and integrin binding sites available on the surface of the molecule.

Heat or chaotrope-induced conformational changes in vitronectin are not limited to alterations in its tertiary structure. In fact, treatment of vitronectin with acid, chaotropic agents, and heat with subsequent refolding produces a multimeric form of vitronectin (Stockmann, *et al.*, 1993). The formation of multimeric vitronectin has been studied extensively (Zhuang, *et al.*, 1996; Bittorf, *et al.*, 1993; Zhuang, *et al.*, 1996). At both physiological pH and ionic strength, the folding and refolding curves of vitronectin exhibit hysteresis (Zhuang, *et al.*, 1996). During refolding, unfolded vitronectin is in equilibrium with a partially folded intermediate, which has been found to have a high propensity to aggregate (fig. 1.5). The refolding pathway favors multimerization under most physiological conditions; however, the direction of the refolding equilibrium can be shifted towards the monomeric species in the presence of high salt concentrations. Salt disrupts electrostatic interactions required for monomeric stabilization and strengthens the intramolecular hydrophobic interactions that stabilize the monomeric species.

The heparin-binding properties of native and multimeric vitronectin have been analyzed more extensively using fluorescence spectroscopy to determine the binding





**Mv**

**V: native, monomeric form**

**V\*: intermediate, partially folded**

**U: fully unfolded monomer**

**Mv: multimeric form**

**Fig. 1-6:** Cartoon illustrating the mechanism by which vitronectin forms higher order, multimeric structures.



constant for the heparin interaction (Zhuang, *et al.*, 1997). This data quantifies the binding constant for the vitronectin-heparin interaction (Zhuang, *et al.*, 1997) and shows that the affinity for heparin is the same for either binding site in the native or multimeric vitronectin. The enhanced binding activity observed in denatured/renatured vitronectin is derived from the alignment of multiple binding sites on the surface of the refolded molecule rather than from increased exposure of the binding sites upon refolding. These studies provide evidence that the heparin considering the effects of multivalency when analyzing functional differences in native vs. multimeric vitronectin. It is incorrect to assume that the augmented affinity of multimeric vitronectin for ligands such as cells, monoclonal antibodies, or collagen results from exposure of neoepitopes without having considered the "Velcro-effect" that stems from clustered binding sites within higher order vitronectin complexes.

**Differential Localization:** Multimeric vitronectin displays a higher effective binding activity towards a broad range of target ligands. Significantly, the stable multimeric conformer is not merely a phenomenon resulting from harsh treatment *in vitro*. Multimeric vitronectin is in fact produced *in vivo*. Vitronectin circulates in plasma predominately in a monomeric state, yet approximately 2% of circulating vitronectin is multimeric (Izumi, *et al.*, 1998). In addition, higher order vitronectin complexes have been detected in the ECM (Stockman, *et al.*, 1993), platelet releasates (Seiffert, *et al.*, 1996), and within the  $\alpha$  granules of platelets (Seiffert, *et al.*, 1996). PAI-1 and heparin have been shown to preferentially bind the ECM form of vitronectin, and platelet vitronectin displays affinity for PAI-1 that closely resemble that of multimeric vitronectin produced by denaturation (Mimuro, *et al.*, 1997; Seiffert *et al.*, 1996).



It is highly unlikely that oligomeric vitronectin is generated *in vivo* via denaturation and renaturation, thus the physiological mechanism of vitronectin multimerization remains a topic of interest. It has been demonstrated that interactions with ligands such as C5b-7 or PAI-1 increase the affinity of vitronectin for glycosaminoglycans, cells, and collagen. The terminal complement complex contains multiple copies of vitronectin, as do TAT complexes (Preissner, *et al.*, 1987; Podack, *et al.*, 1979). It has recently been demonstrated that PAI-1-vitronectin complexes harbor more than a single molecule of vitronectin (Declereck, *et al.*, 1988; Peterson, *et al.*, 1998;). Thus, interaction with target ligands could possibly result in multimerization of vitronectin.

Because vitronectin preferentially interacts with both collagen and elastin, conformationally altered vitronectin may be preferentially deposited in the matrix. A study has shown that conformationally altered vitronectin produced *in vitro* binds to endothelial cells in a glycosaminoglycans-dependent manner (de Boer, *et al.*, 1992). By localizing vitronectin with immunogold, it was shown that multivalent forms of vitronectin were transcytosed by cells and incorporated into the matrix (Volker, *et al.*, 1993). The multimeric form of vitronectin is also preferentially endocytosed by fibroblasts (Panetti, *et al.*, 1993; Panetti, *et al.*, 1995; Panetti, *et al.*, 1993). The  $\alpha_v\beta_5$  receptor mediates the endocytosis of ECM vitronectin. Within fibroblasts, vitronectin is degraded, which suggests a role for the fibroblast integrin receptors in tissue remodeling.

Differential localization of the two forms of vitronectin may serve as a mechanism for regulating the function of the protein within different physiological environments. Once incorporated within the matrix, oligomeric vitronectin may localize



inflammatory, thrombotic, or fibrinolytic proteins to sites of injury at the endothelial vessel wall.

**Enzymatic Modification:** Studies indicate that vitronectin activity may be controlled by intracellular or extracellular proteolysis. For example, when vitronectin is complexed with TAT, it is selectively endocytosed and degraded within fibroblast cell lines, revealing a mechanism through which spent vitronectin might be removed from circulation. Extracellular proteolytic events may be effective for controlling vitronectin function as well. Cleavage of vitronectin with specific proteases such as thrombin and plasmin attenuates binding activity for glycosaminoglycans, and perhaps for other ligands as well. Plasmin degraded vitronectin has a high affinity for plasminogen. This high affinity may suggest a feedback loop mechanism for controlling activity at the site of wound healing. Plasma vitronectin normally would exhibit a prothrombotic effect by sustaining coagulation and inhibiting fibrinolysis. Plasmin and thrombin are highly concentrated in the vicinity of the thrombus. These proteases could cleave susceptible sites on vitronectin, attenuating heparin and PAI-1 binding function, thereby allowing clot lysis to continue. Moreover, plasminogen would be localized to the site of the vessel wall under such circumstances where it could be activated to degrade the fibrin clot.

Matrix metalloproteinases-2, -3, -7 and -9 also degrade vitronectin (Imai, *et al.*, 1995). These proteases degrade ECM components like collagen, fibronectin, and laminin. The functional significance of the degradation has not been demonstrated, but it is likely to be important for ECM remodeling. Vitronectin induces MMP-2 expression in melanoma cells via the  $\alpha_v\beta_3$  integrin receptor (Sefter, *et al.*, 1993). This vitronectin-induced MMP-2 stimulation would explain the invasive properties of cancerous cells.



The overexpressed MMP-2 would degrade vitronectin and other matrix components, thereby releasing tumor cells from the matrix.

A platelet membrane protease has also been shown to degrade vitronectin. Calpains I and II are expressed on the surface of platelet membranes (Kambayashi, *et al.*, 1989). Upon membrane damage induced by freeze thaw methods or by addition of nonionic detergent, calpain activity was stimulated, degrading both platelet and exogenously applied vitronectin (Seiffert 1996). Limited digestion with calpain reduced the PAI-1, heparin, and cell binding activities of vitronectin. Thus, platelet injury made lead to proteolytic events that reduce vitronectin activity.

Interestingly, endogenous proteolytic cleavage of vitronectin occurs at position 44 (releasing the somatomedin B domain) and at position 379; however, not all vitronectin is susceptible to the C-terminal cleavage. A genetic polymorphism at position 381 determines the sensitivity of vitronectin to proteolysis at this position. The presence of methionine at position 381 is associated with single-chain vitronectin, whereas threonine at position 381 increases the susceptibility to cleavage at the 379-380 peptide bond (Tollefsen, *et al.*, 1990). Each of the alleles is present at a frequency of approximately 50% in white populations (Conlan, *et al.*, 1988). Approximately 18% of people are homozygous for the single chain vitronectin allele, and 22% are homozygous for two-chain vitronectin. Heterozygotes represent 59% of the population. While endogenous removal of the somatomedin B domain has been shown to decrease affinity for PAI-1 (Sigurdardottir, *et al.*, 1994), it is not known whether cleavage at 379 affects vitronectin activity.



Post-translational chemical modification of vitronectin may also play a role in regulating its activity. Protein kinase A dependent serine phosphorylation occurs within the heparin binding sequence of vitronectin both *in vitro* and *in vivo*. It has been suggested that the phosphorylated form of vitronectin may exhibit altered binding activity towards ligands that bind to the arginine-rich C-terminal sequence (Gechtman, *et al.*, 1997; Chain, *et al.*, 1990; Sane, *et al.*, 1991; Preissner, *et al.*, 1990; Peake, *et al.*, 1996). Treatment of vitronectin with factor XIIIa or transglutaminase *in vitro* results in the formation of covalently-crosslinked multimers, which display increased affinity for PAI-1.

### **Computational Model**

We recently proposed a model of vitronectin using computational methods ( Xu, *et al.*, 2001). In this approach, we adopted the domain assignment described previously for the N-terminal, central and heparin-binding domains, and predicted the structure of each domain separately. Fold recognition through sequence-structure alignment (threading) ( Xu, *et al.*, 1998) was used for the structural modeling. The predicted structures for the three domains using this method are shown in Fig.1-7, Panels a, b and c. As shown in the linear schematic of vitronectin in Fig. 1-7d, the structural models for the domains do not include the connecting region between the N-terminal and central domains, which is predicted to be highly unstructured.

The central domain (residues 129-323) is modeled as a full 4-bladed  $\beta$ -propeller fold similar to that seen in gelatinase A (Gohlke, *et al.*, 1996), collagenase ( Gomis-Ruth, *et al.*, 1996) and hemopexin ( Faber, *et al.*, 1995). The threading results for the C-



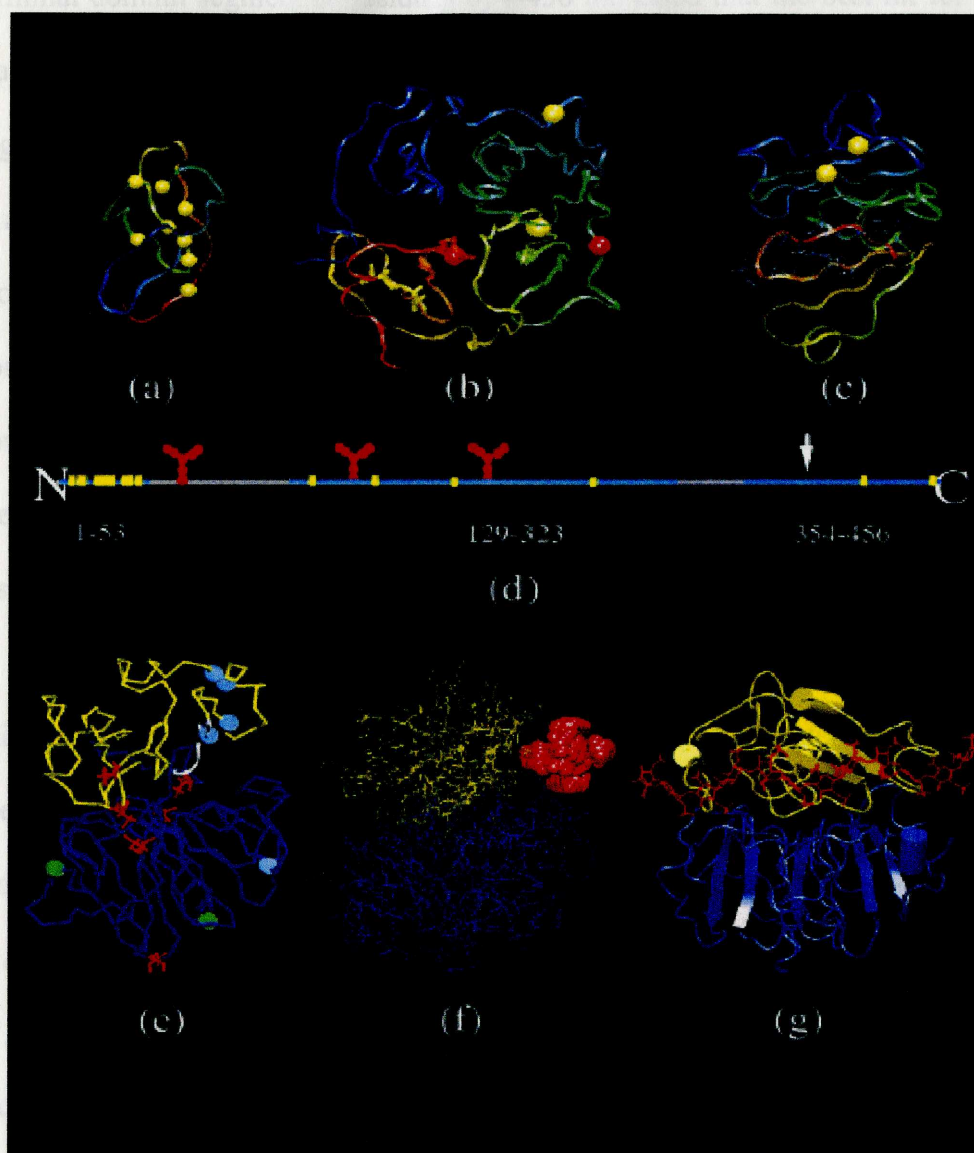


**Fig. 1-7:** Structural models of vitronectin. (a-c) show the structural models of the N-terminal somatomedin B domain, the central domain with a four-bladed b-propeller fold, and the C-terminal heparin-binding domain, respectively. The color from the red to blue shows the sequence order from the N-terminus to the C-terminus. The yellow solid spheres indicate cysteines. White spheres (a) show the integrin attachment site; red spheres (b) show glycosylation sites (residues 150 and 223); and thin lines (c) show the heparin-binding site. d: Linear representation of the sequence of vitronectin, with blue highlighting corresponding to domains modeled in (a-c), yellow dots indicating cysteines, red structures representing carbohydrate attachment sites, and the white arrow pointing to the known site of protease cleavage to the two-chain form. e: Docking structure between the central (blue) and C-terminal (yellow) domains, with cysteines (red lines), presumed heparin-binding residues (354-363 in white ribbons), sites susceptible to protease (residues 305, 361, 370, 379 and 383 with light blue spheres), and N-linked glycosylation sites (residues 150 and 223 with green spheres). f,g: Predicted docking the N-terminal, central and heparin-binding domains, and predicted the structure of each domain separately.



terminal domain segment of residues 354-456 indicated that the best hit for this domain was also the PDB entry *Igen* (C-terminal end of gelatinase A). However, the sequence segment covers only half of the 4-bladed  $\beta$ -propeller fold. The threading method, which is an algorithm that samples all of the structural entries in the PDB to arrive at a given model (Xu, *et al.*, 2001; Xu, *et al.*, 1998), thus agrees with the early report of distant homology with hemopexin based on patterns within the repeated sequence motifs that we now know comprise the propeller blades (Jenne, *et al.*, 1987). The predicted structure for the N-terminal domain (residues 1-53) is an open 5-stranded  $\beta$ -barrel fold that is rich in disulfide bonds.

In further work, we have docked the central and C-terminal domains together to gain insight into the overall fold of the protein (Fig 1-7e). An inter-domain disulfide was used to constrain the docking, and our model was tested for agreement with numerous biochemical results. In particular, the orientation of the heparin-binding domain (Gibson, *et al.*, 1999), burial of known free sulfhydryls (Zhuang, *et al.*, 1996), and the positioning of glycosylation sites (Ogawa, *et al.*, 1995) were considered. The known heparin-binding sequence appears in the model to lie within a groove between the two domains, with suitable dimensions for binding of heparin. Two positively charged arginine residues lie at the base of this binding pocket; we have shown that these two residues exhibit intermolecular nuclear Overhauser effects (NOEs) with heparin in nuclear magnetic resonance (NMR) experiments with a peptide from the heparin-binding region from vitronectin (Gibson, *et al.*, 1999). The participation of the two domains to form the heparin-binding site in the model is consistent with a report using recombinant fragments from vitronectin that assigns weak heparin-binding function to the central domain



(Yoneda, *et al.*, 1998). To test this predicted binding site, we also docked heparin together with the two-domain protein model (Fig. 1-7, Panels f and g) and observed a good fit of the ligand in the binding pocket. These modeling results are compelling and provide impetus for an experimental confirmation of the predictions.

## Chapter 2

### CRYSTALLIZATION/CO-CRYSTALLIZATION OF FULL-LENGTH, NATIVE, MONOMERIC VITRONECTIN

#### Introduction

Human vitronectin has the intriguing capability of interacting with a broad spectrum of ligands, which in turn gives it the ability to regulate an array of physiological processes. The form of vitronectin found in circulation is important in pathological situations or in cancer metastasis and tissue remodeling by its association with the vascular extracellular matrix. Presently, a thorough understanding of the control mechanisms governing vitronectin's macromolecular binding and therefore its characteristic activities both in circulation and the ECM is still being sought after empirically.



Research within our lab is based on several hypotheses: Vitronectin is a multi-domain protein with distributed binding sites to control the dynamic processes of coagulation vs. fibrinolysis and binding vs. release from the matrix. Complexes of vitronectin with biological targets associate into higher-order structures with altered functions and tissue compartmentalization. Vitronectin complexes are recognized by cell-surface receptors, with a preference for higher-order complexes over free, monomeric vitronectin.

**Chapter 2** investigations into vitronectin structure/function relationship, a model has emerged in which vitronectin is organized into several domains that provide the extensive repertoire of binding epitopes for target ligands. As our lab has progressed in ligand-

## **CRYSTALLIZATION/CO-CRYSTALLIZATION OF FULL-LENGTH, NATIVE, MONOMERIC VITRONECTIN**

### **Introduction**

Human vitronectin has the intriguing capability of interacting with a broad spectrum of ligands, which in turn gives it the ability to regulate an array of physiological processes. The form of vitronectin found in circulation is important in pathological situations or in cancer metastasis and tissue remodeling by its association with the vascular extracellular matrix. Presently, a thorough understanding of the control mechanisms governing vitronectin's macromolecular binding and therefore its characteristic activities both in circulation and the ECM is still being sought after empirically.



Research within our lab is based on several hypotheses: Vitronectin is a multi-domain protein with distributed binding sites to control the dynamic processes of coagulation vs. fibrinolysis and binding vs. release from the matrix. Complexes of vitronectin with biological targets associate into higher-order structures with altered functions and tissue compartmentalization. Vitronectin complexes are recognized by cell-surface receptors, with a preference for higher-order complexes over free, monomeric vitronectin.

From investigations into vitronectin structure/function relationship, a model has emerged in which vitronectin is organized into several domains that provide the extensive repertoire of binding epitopes for target ligands. As our lab has progressed in ligand-binding work, we have realized the value of a structural model in guiding our understanding of vitronectin and its interactions with target molecules. We recently proposed a structural model of vitronectin using computational methods (threading). These modeling results are compelling and provide impetus for an experimental confirmation of the predictions. I have focused my research primarily on the crystallization of vitronectin, for as encouraging as the computational predictions for vitronectin structure are, we are cautious and must validate the model experimentally.

Crystallization is a way by which a metastable, supersaturated solution can reach a stable, lower energy state via reduction of solute concentration (Weber, *et al.*, 1991). Relative to their state in solution, crystallization generally lowers the free energy of proteins by approximately 3-6 kcal/mole (Drenth, *et al.*, 1992). The general processes by which substances crystallize are similar for molecules of both microscopic (salts) and



macroscopic (proteins) dimensions. There are three stages of crystallization common to all systems: 1) nucleation, 2) growth, and 3) growth termination.

It is entirely by chance that solvated molecules will associate at any given time with the appropriate geometric orientations required to form an aggregate nucleus. After this event is achieved, however, the newly formed nucleus can serve as a platform on which further protein macromolecules can be adsorbed and geometrically aligned to form an ordered crystal lattice. After crystallization has been initiated, it is not ensured that the crystal will inevitably continue to grow. The probability of crystal growth is dependent upon such factors as solute concentration, temperature, the nature of the chemical used to induce precipitation, pH, as well as other physical and chemical factors. The concentration of successfully formed nuclei directly affects the outcome of crystallization. Conditions that induce the formation of only a few nuclei must be achieved in order to produce crystals suitable for subsequent X-ray diffraction studies (0.1-0.3 mm).

The nucleation event involves the association of solvated molecules or non-crystalline aggregates (i.e. oligomers) in a manner that produces a thermodynamically stable aggregate with a characteristic repeating lattice. Nucleation from supersaturated protein solutions does not always necessitate formation of macroscopic crystals. The protein aggregate must first exceed a critical size defined by its surface area to volume ratio (Feher, *et al.*, 1985; Boistelle, *et al.*, 1988). Having met this size-dependent criterion, the aggregate nucleus is then capable of further growth. If at any time, however, the nucleus falls beneath this critical size, it will spontaneously dissolve. The phenomenon of amorphous precipitation does not involve surface area to volume



competition, and so it generally takes significantly less time to occur relative to crystallization.

The degree of nucleation is determined by the degree of solute supersaturation. Moreover, the extent of supersaturation is in turn related to the protein's overall solubility. Higher solubility allows for an increased frequency of diffusional collisions. Higher degrees of supersaturation produce more stable aggregates and will therefore increase the likelihood of stable nuclei formation. This condition generally facilitates excessive production of small crystals in solutions in which solute molecules are overly available. In this case, there will be a depletion of solvated protein available for association making the attainment of large, diffraction quality species impossible. At lower solute concentrations, however, the frequency with which individual, stable nuclei are formed decreases, and the formation of individual crystals is favored.

Molecular deposition onto the nucleus is an exceptionally dynamic process. The more specific interactions a solvated protein molecule forms as it associates with the growing crystal, the tighter will the binding be as a result of a lower free energy of formation. A low energy value will in turn give rise to greater crystalline stability.

Successful protein crystallization depends highly on the purity of the sample being used. Due to the use of small volumes in the vapor diffusion method, any impurities within a sample will be present in relatively high concentration leading to contamination of the crystal lattice and ultimately poor crystals.



### Problems:

Crystallization assumes that *identical*, macromolecular protein units are available within the drop to be incorporated into an ordered crystal lattice. A significant problem in obtaining crystallographic/structural information for native vitronectin comes from the inability to acquire a homogeneous sample due to factors such as proteolytic cleavage, glycosylation, phosphorylation, and formation of higher order species.

Vitronectin is purified from pooled human plasma that contains both single and double chain structural forms (Zhuang, *et al.*, 1997). In vivo, vitronectin can exist in a full-length or a two-chain, cleaved form. Cleavage occurs by an unidentified trypsin-like protease, which cuts vitronectin just beyond the heparin-binding domain at arginine 379 (Tollefsen, *et al.*, 1990). The presence of threonine versus methionine at position 381 increases the likelihood that vitronectin will be cleaved at position 379. The cleaved molecule is a two-chain form of vitronectin: a 62 kDa N-terminal heavy chain and a 10 kDa C-terminal light chain. A single disulfide bond holds the two chains together. The 72 kDa and 62 kDa forms of vitronectin can be seen on the Coomassie-stained SDS-PAGE gel in figure 2-1, panel A, and on the reversed-phase HPLC chromatograph, panel B. Although it is generally assumed that the two forms of vitronectin are functionally indistinguishable, this premise has not been proven empirically.

The formation of crystal lattice contacts (Fig. 2-2, panel A) relies heavily on protein sample homogeneity. In a heterogeneous sample, the protein will be less



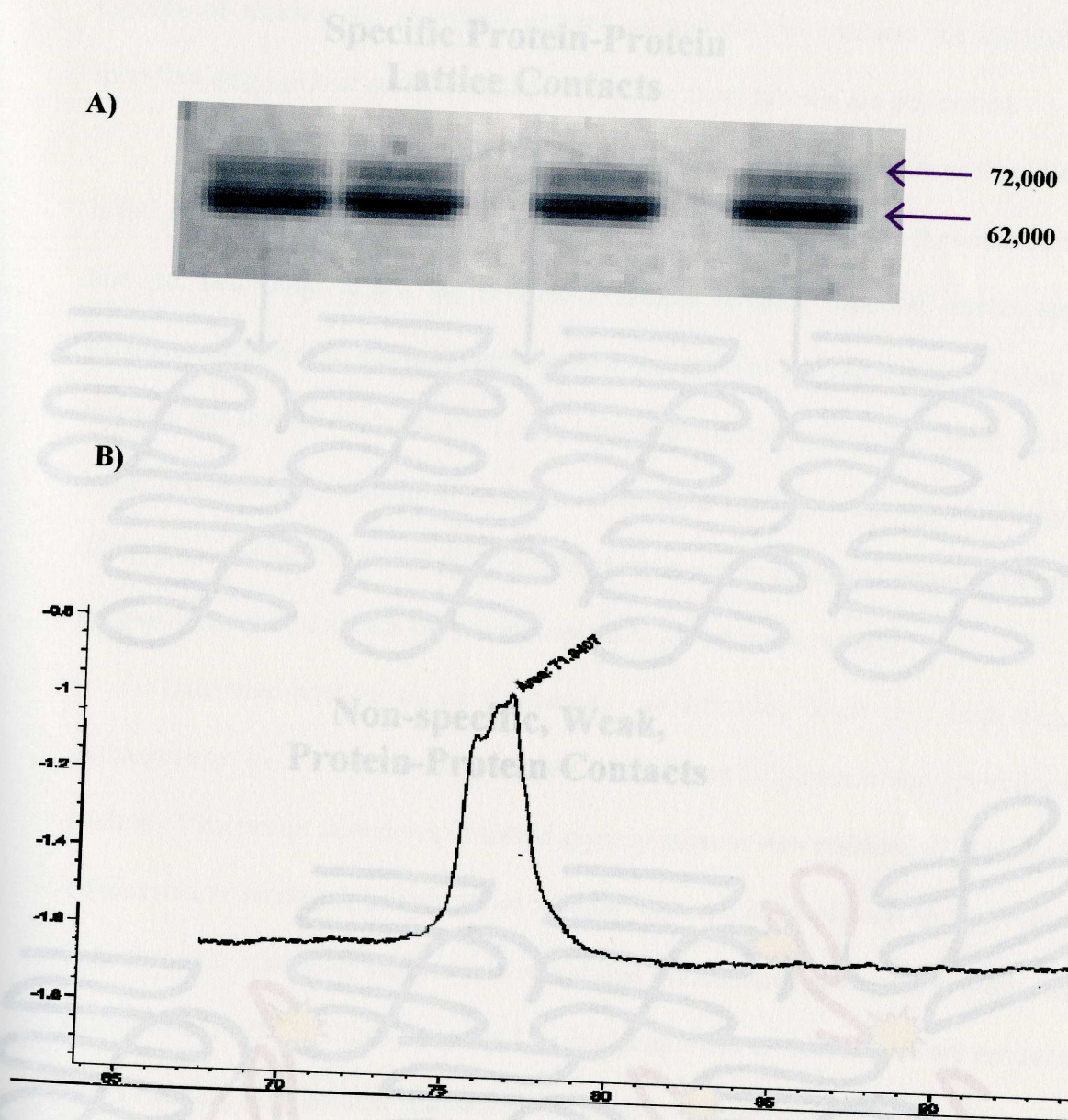
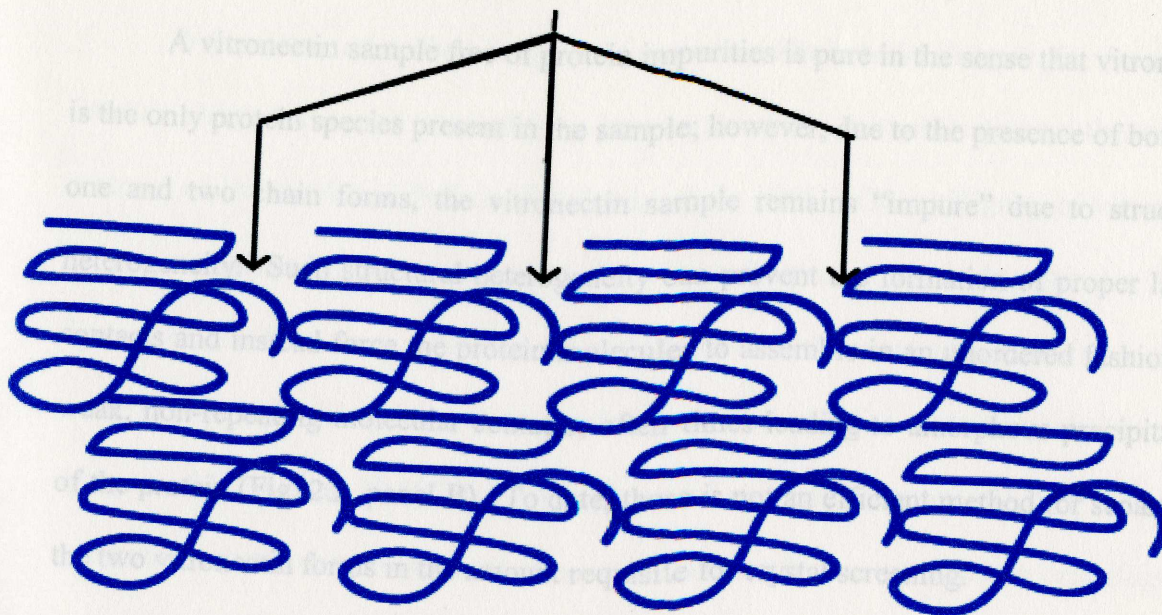


**Fig. 2-1:** Panel A: A 10% SDS-PAGE Coomassie-stained gel shows the presence of the 72 kDa and 62 kDa forms of vitronectin. Panel B: the 72 kDa and 62 kDa forms of vitronectin seen by reversed-phase HPLC.



## Specific Protein-Protein Lattice Contacts



## Non-specific, Weak, Protein-Protein Contacts

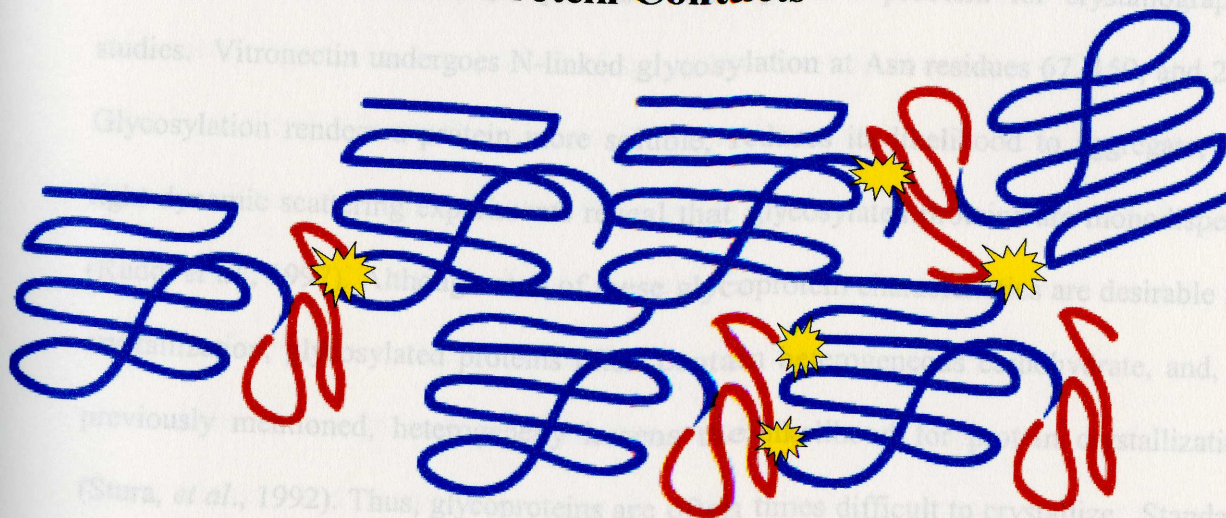


**Fig. 2-2:** Panel A illustrates stabilized, repeating, protein-protein lattice contacts requisite for crystal formation and subsequent growth. Panel B illustrates the weak, non-repeating, protein-protein contacts (yellow), which arise from structural heterogeneity (one and two chain structural forms) of the protein sample.



capable of making the necessary ordered protein-protein contacts for nucleation and therefore may never crystallize regardless of how many screens are performed.

A vitronectin sample free of protein impurities is pure in the sense that vitronectin is the only protein species present in the sample; however, due to the presence of both the one and two chain forms, the vitronectin sample remains "impure" due to structural heterogeneity. Such structural heterogeneity can prevent the formation of proper lattice contacts and instead force the protein molecules to assemble in an unordered fashion via weak, non-repeating molecular contacts, often times leading to amorphous precipitation of the protein (Fig. 2.2, panel **B**). To date, there is not an efficient method for separating the two vitronectin forms in the amount requisite for crystal screening.

Extensive post-translational, chemical modification leads to a high degree of heterogeneity in vitronectin samples and thus poses a problem for crystallographic studies. Vitronectin undergoes N-linked glycosylation at Asn residues 67, 150, and 223. Glycosylation renders a protein more soluble, reduces its likelihood to aggregate, and light dynamic scattering experiments reveal that glycosylated proteins are monodisperse (Rudd, *et al.*, 1997). Although each of these glycoprotein characteristics are desirable for crystallization, glycosylated proteins often contain heterogeneous carbohydrate, and, as previously mentioned, heterogeneity lessens the likelihood for protein crystallization (Stura, *et al.*, 1992). Thus, glycoproteins are often times difficult to crystallize. Standard enzymatic and chemical methods for removing protein carbohydrate were extensively employed with vitronectin without success. Nevertheless, crystal screens were still performed.



## Experimental Procedures:

### *Preparation of a Full-Length, Monomeric Vitronectin Sample for Screening*

**Studies:** Vitronectin was purified from human plasma by a modification of the original protocol of Dahlback and Podack (Dahlback, *et al.*, 1985). One milligram of vitronectin from a precipitated ammonium sulfate slurry was dialyzed extensively against a .02 M Tris, .1 M NaCl solution, pH 7.4 at 4°C. Purity of the vitronectin sample was analyzed using SDS-PAGE. The vitronectin sample was concentrated to approximately 10 mg/ml using a .5 Ultrafree 30,000™ MWCO centrifugal concentration device. Prior to screening, any amorphous material present in the sample was removed by centrifugation at 10,000 RPM at 4°C.

**Crystal Screening:** Screening of crystallization conditions for full-length, monomeric vitronectin was performed using the hanging-drop vapor-diffusion method using both Crystal Screen™ and Index™ crystal screens commercially available from Hampton Research. Crystal Screen™ is a 50 condition, sparse matrix-based crystal screen that allows the testing of wide ranges of pH, salts, and precipitants using a very small sample of macromolecule (Jancarik, *et al.*, 1991).

Index™ is a 96 reagent screen that combines the strategies of the grid screen, sparse matrix, and incomplete factorial with classical, contemporary, and novel crystallization reagent systems. Index™ samples the classical and often effective reagent ammonium sulfate in a grid screen format across a pH range of 3.5 to 8.5. Classical salts such as sodium chloride, phosphate, and formate are also sampled across a broad range of pH.



The concentration of vitronectin samples used for crystal screening were between 10 and 15 mg/ml as determined by absorption at 280 nm. All screens were performed at 4°C to prolong vitronectin stability within the drop. 24-well VDX™ plates purchased from Hampton Research were prepared for hanging drop vapor diffusion by applying vacuum grease around the edges of the reservoirs. 1000 µl of each screening reagent was pipetted into the VDX™ plate reservoirs. 1.0 µl of concentrated vitronectin was pipetted onto the center of a 22 mm siliconized, circle cover slide, and 1.0 µl of screening reagent was subsequently removed from each reservoir and pipetted into the protein sample droplet on the siliconized cover slide. Instead of adding the vitronectin drop to the precipitant drop, precipitant was added to the vitronectin drop so as to avoid precipitation due to the sudden exposure of vitronectin to a very high precipitate concentration. Cover slides were then inverted, placing the droplets over the reagent reservoirs, and the cover slides were sealed to the reservoirs' edges.

**Screen Drop Interpretation:** Each of the crystallization experiments was examined using a stereomicroscope immediately after setting up each screen, everyday for one week following the setup, and once a week thereafter. Each individual drop was examined and all observations were recorded. I chose to simplify my data record keeping by adopting a one number drop scoring method described by Bergfors, *et al.*, wherein a numerical score (1-9) is recorded for each drop condition within a screen. Figure 2-3 illustrates the numerical representation used to score the large number of screen conditions.



During the screening for vitronectin crystallization conditions, any drops observed that remained clear (score of 0) for a period longer than two weeks were removed and placed over a reservoir containing the same condition but with a higher precipitant

| <u>Score</u> | <u>Drop Phenomena</u>                                  |
|--------------|--|
| (0)          | - clear drop   |
| (1)          | - non-proteinaceous particle (glass/fibers)            |
| (2)          | - light precipitation/drop mostly clear                |
| (3)          | - fully precipitated protein                           |
| (3)          | - precipitation upon mixing with viscous well solution |
| (3)          | - wrinkled skin/denatured protein                      |
| (4)          | - gelatinous protein-precipitate                       |
| (4)          | - gelatinous protein                                   |
| (5)          | - phase separation                                     |
| (6)          | - spherulites  |
| (6)          | - transparent cluster                                  |
| (6)          | - microcrystals  |
| (7)          | - needles  |
| (8)          | - plates   |
| (9)          | - crystals   |

**Fig. 2-3:** Numerical representations for crystal screen condition scoring.



protein During the screening for vitronectin crystallization conditions, any drops observed that remained clear (score of 0) for a period longer than two weeks were removed and placed over a reservoir containing the same condition but with a higher precipitant concentration. Drops that, after two weeks, were mostly clear but contained precipitated vitronectin (score of 2) were recorded so as to avoid repeating these particular conditions in future screens. The rationale for avoiding these conditions in future screens is that either the vitronectin or precipitate concentrations within these drops most likely does not favor nucleation/crystal growth. Dark drops in which vitronectin fully precipitated (score of 3) within one day were recorded so that these conditions could be repeated in future screens with half the precipitate concentration. Conditions containing heavy vitronectin precipitate after approximately one week do not favor crystallization and were avoided in future vitronectin screens.

### Results and Discussion:

Four vitronectin crystal screens were performed using Crystal Screen™, two with a 10 mg/ml vitronectin sample and two with a 15 mg/ml sample. In addition, two Index™ screens were performed using one 10 mg/ml vitronectin sample and one 15 mg/ml sample. Condition 19 of Crystal Screen™ (0.2 M Ammonium Acetate, 0.1 M Tris Hydrochloride pH 8.5, 30% v/v iso-Propanol) produced 3 micron x 3 micron microcrystals, which ceased growing after approximately four weeks. Attempts to optimize around this condition have not yet been performed due to scarcity of protein.

The majority of conditions in both Crystal Screen™ screens produced amorphous precipitate within the first week for both vitronectin concentrations screened. Index™ produced a number of conditions containing protein gel mixtures and spherulites in both



protein concentrations screened; therefore Index™ screen shows more promise for vitronectin crystallization than does Crystal Screen™, for full vitronectin precipitation was observed in only approximately 55% of the conditions.

### **Vitronectin Co-crystallization**

**Rationale:** Sparse matrix crystal screening generally yields crystals only for proteins that crystallize with facility. Such proteins are capable of readily forming the stable protein-protein interactions requisite for crystal lattice formation. Unfortunately, a large proportion of proteins do not fall within this category. By increasing the number of crystallization trials, diminished returns are reaped such that the augmented effort is difficult to justify. Because vitronectin has been such a difficult protein to crystallize, the possibility of employing a *scaffold* for protein crystallization becomes enticing. One such scaffold approach is based upon the use of immunoglobulin (IgG) fragments, wherein the protein of interest is the antigen recognized by the IgG. The system envisaged is one consisting of approximately two stages: 1) the screening for an appropriate scaffold IgG fragment, and 2) the optimization of the scaffold system for diffraction quality crystals.

Immunoglobulins are known to create a specific and stable complex with the epitope of their target protein and, owing to their high affinity, are used as a tool for Enzyme Linked Immunosorbant Assay (ELISA) and Western blotting analysis to detect tiny amounts of protein. The tertiary structures of IgG antigen-binding fragments complexed with antigens have been investigated in detail (Silverton, et al., 1984; Laver, et al., 1990; Ostermeier, et al., 1995).



Fab and F(ab)<sub>2</sub> fragments can be used as co-crystallization agents even in the crystallization of highly deterrent membrane proteins (fig. 3-1) (Ostermeier, *et al.*, 1995). Such antibody fragments are very soluble and bind specifically to antigens with reasonable equilibrium constants. IgG fragments can, in some instances, effectively transform aggregated protein into a soluble, monodispersed protein sample suitable for crystallization trials. It has also been found that IgG fragments can immobilize a region of a protein thereby reducing sample flexibility and enhancing sample conformational homogeneity, which enhances chances for crystallization (Stura, *et al.*, 2001a). With recent improvements in the use of molecular replacement (MR), the structure determination of IgG-antigen complexes can proceed at a relatively quick pace. For this project, crystallization of vitronectin and subsequent structure determination is directed primarily towards the use of Fab fragments as a co-crystallization agent. The rationale behind the use of Fab fragments remains linked both to the ease with which the structure of Fab fragments have been determined and to the difficulties that have been presented by the crystallization with either whole IgG or other IgG fragments (Haynes, *et al.*, 1994; Zhou, *et al.*, 1994). This difficulty is believed to be due to the flexibility or conformational heterogeneity of the IgG due to the various disulfide-linked chains as well as to added heterogeneity from Fc fragment glycosylation. F(ab)<sub>2</sub> fragments share some of the same problems mainly because of the degree of heterogeneity that may result from proteolytic cleavage used to fragment the IgG, the flexibility in elbow regions, and in some cases glycosylation. Nevertheless, F(ab)<sub>2</sub> fragments, specifically their reduced F(ab)' form, have been shown to serve as successful scaffolds for protein crystallization



and therefore will be used in addition to Fab fragments as a scaffold candidate for vitronectin crystal screens (Fig. 3-2).

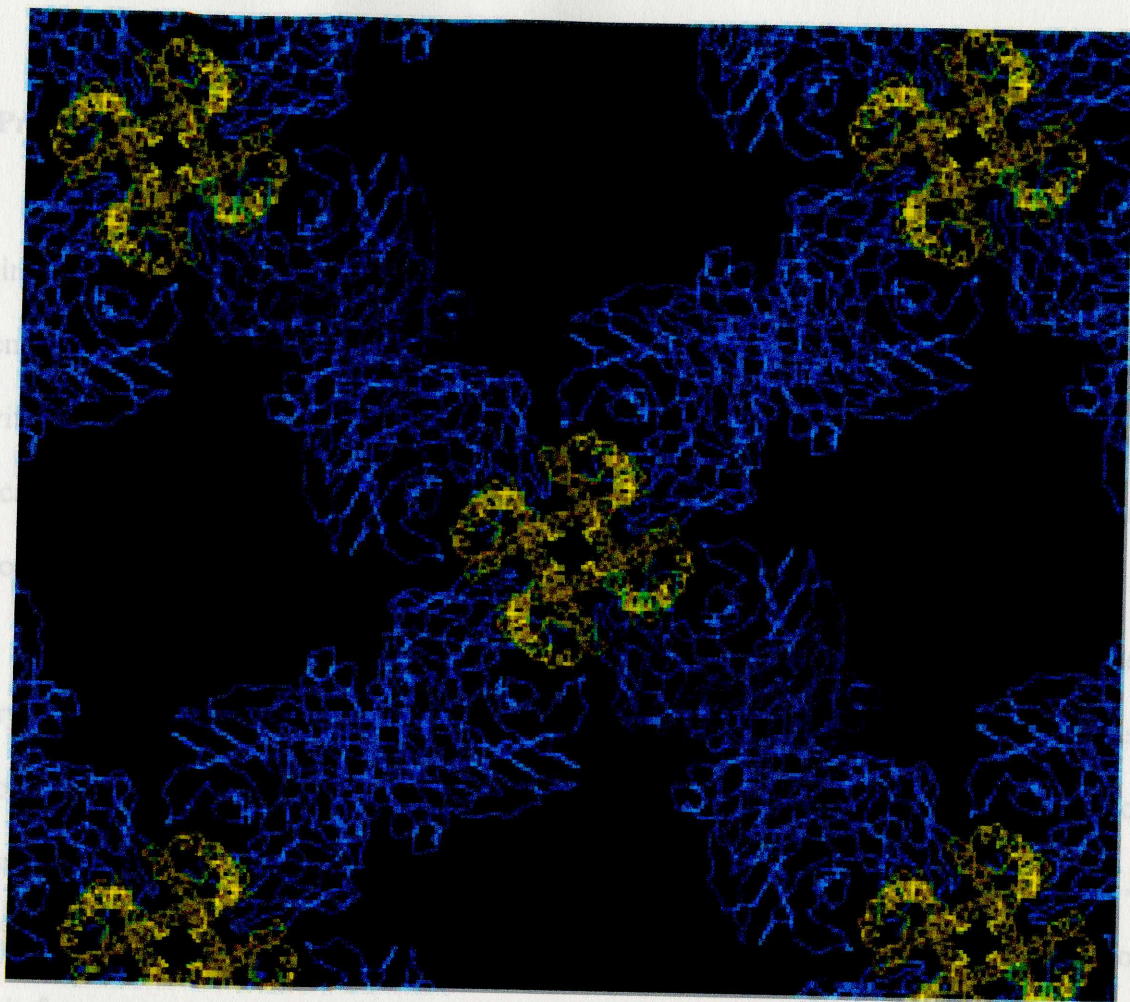


**Fig. 3-1: Antigen-Fab Crystal Packing.** KcsA (yellow) was crystallized as a complex with an antibody Fab fragment (blue) at 2.8Å resolution. The image is a view down the four-fold crystallographic axis of the I4 cell, which corresponds to the molecular four-fold axis of the K<sup>+</sup> channel (Zhou, *et al.*, 2001).

direction which in the complex replicates the packing found in crystals of the uncomplexed Fab (Stura, *et al.*, 2001b). Changing the stoichiometry alleviates size and polymerization problems: as the complex gets larger, the concentration of scaffold protein is increased. In the Fab 2A2-SpA example (Graille, *et al.*, 2000), the free Fab in the lattice of the 2A2-SpA complex packed along one lattice direction in the same



and therefore will be used in addition to Fab fragments as a scaffold candidate for vitronectin crystal screens (fig. 3-2).

### Problems

Theoretically, the size of a protein that can be accommodated by the scaffold is limited, even in one-dimension. Furthermore, the size of the protein must be small enough so as to not disturb the packing of the scaffold. For example, a protein such as vitronectin that forms multimeric complexes could disrupt the correct alignment of the scaffold. In light of this problem, stoichiometry variation of the vitronectin-IgG fragment complex will be performed in screening as described by Stura, *et al.*, 2001b.

An example of the stoichiometry variation phenomenon was found in the crystallization of Fab 2A2 in complex with protein SpA. In the crystallization of this complex, Stura, *et al.* found that the addition of extra scaffold proteins helped to overcome problems that arose when the added SpA protein dimerized (Stura, *et al.*, 2002). The crystals of the Fab 2A2-SpA complex showed a 3:2 stoichiometry with two Fab fragments complexed and one free (Graille, *et al.*, 2000). The two SpA molecules dimerized and forced the dimerization of two of the three Fabs in the asymmetric unit. Without the extra copy of Fab 2A2, it would not be possible to maintain the "scaffold" direction which in the complex replicates the packing found in crystals of the uncomplexed Fab (Stura, *et al.*, 2001b). Changing the stoichiometry alleviates size and polymerization problems: as the complex gets larger, the concentration of scaffold protein is increased. In the Fab 2A2-SpA example (Graille, *et al.*, 2000), the free Fab in the lattice of the 2A2-SpA complex packed along one lattice direction in the same



manner as it did in the crystal of uncomplexed 2A2 suggesting that one-dimensional scaffolds could be generated as the stoichiometry is varied. Unfortunately, a one-dimensional scaffold does not exist.

To make the transition from a one-dimensional scaffold to one of three dimensions, the number of Fab molecules must be increased. To make the transition from a one-dimensional scaffold to one of three dimensions, the number of Fab molecules must be increased. To make the transition from a one-dimensional scaffold to one of three dimensions, the number of Fab molecules must be increased.

IgG Antibody structure. IgG proteins are composed of two heavy chains and two light chains. The fold of the immunoglobulin domain is a highly conserved motif. The Fab portion is

**Fig. 3-2:** Location of the Fab molecules in the P21 crystal lattice of the TPO163-Fab complex. Light-colored Fab molecules and dark colored Fab molecules are anti-parallel. The box indicates the unit cell (Kraulis, 1991).

fragment is made up of four constant domains. The variable and constant domains have similar structures, but the variable domains have two extra  $\beta$ -strands (Rousseaux, *et al.*, 1983). The variable regions were named based on their regions of hypervariable amino



manner as it did in the crystal of uncomplexed 2A2 suggesting that one-dimensional scaffolds could be generated as the stoichiometry is varied. Unfortunately, a one-dimensional scaffold does not exist.

To make the transition from a one-dimensional scaffold to one of three dimensions, there must be some propensity within the system to create the other remaining lattice interactions. With an increase in the number of directions, the number of restrictions increases as well. In a two dimensional case, translational and rotational symmetries must be respected in both dimensions. A "guest" antigen that does not respect such constraints is likely to disrupt the integrity of the scaffold. Thus, screening for the correct IgG fragment scaffold with which to crystallize vitronectin will be carried out in order to determine a suitable scaffold lattice for vitronectin.

### **IgG Antibody structure**

An IgG molecule is made up of two Fab fragments responsible for antigen binding and one Fc fragment responsible for activation of complement. Figure 3-3 illustrates a space filling model of a murine IgG<sub>2a</sub> molecule with its Fab and Fc fragments labeled. IgG proteins are composed of two heavy chains and two light chains. The fold of the immunoglobulin domain is a highly conserved motif. The Fab portion is composed of two variable and two constant domains (Rousseaux, *et al.*, 1983). The Fc fragment is made up of four constant domains. The variable and constant domains have similar structures, but the variable domains have two extra  $\beta$ -strands (Rousseaux, *et al.*, 1983). The variable regions were named based on their regions of hypervariable amino



**Fab** **Fab**

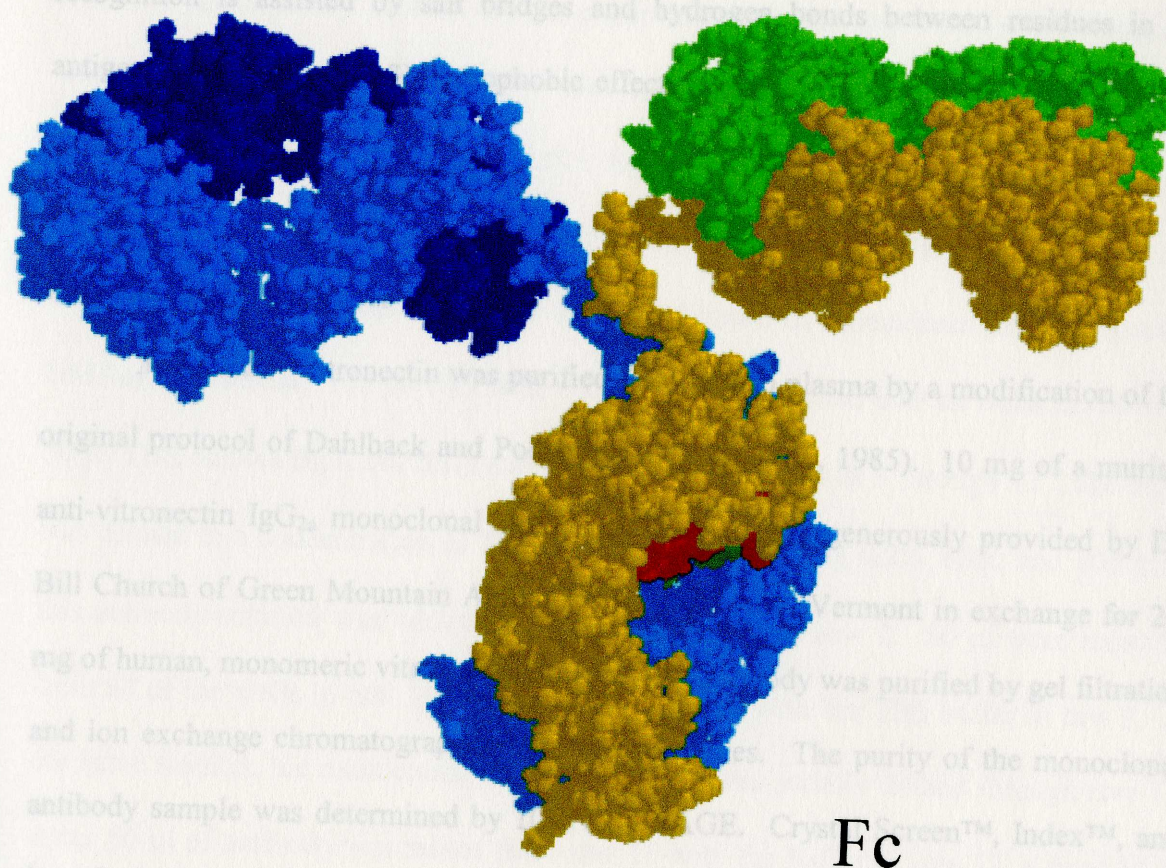


**Fig. 3-3:** The image is a space filling model of mouse IgG<sub>2a</sub>. The two heavy chains are shown in yellow and light blue whilst the two light chains are shown in green and dark blue. The carbohydrate (red and green) is visible in the Fc fragment (Harris, *et al.*, 1997).

**Determining the Titer of GMA<sub>104</sub> Monoclonal Antibody via ELISA:** Vitronectin was purified from human plasma by a modification of the original protocol of Dahlback and Podack (Dahlback, *et al.*, 1985). A microtiter plate was coated with a 5 µg/ml vitronectin solution in 50 mM sodium carbonate (NaCO<sub>3</sub>), pH 8.5 as the coating buffer.



acid sequence, which correspond to the antigen-binding site. In all Fab/antigen structures studied so far, the following general observations have been made. 1) Good structural complementarity exists between the binding surfaces of antibody and antigen; 2) recognition is assisted by salt bridges and hydrogen bonds between residues in the antigen binding site; and 3) hydrophobic effects and water molecules may play a role in recognition.

## Experimental Procedures

**Materials:** Vitronectin was purified from human plasma by a modification of the original protocol of Dahlback and Podack (Dahlback, *et al.*, 1985). 10 mg of a murine, anti-vitronectin IgG<sub>2a</sub> monoclonal antibody (GMA<sub>900</sub>) was generously provided by Dr. Bill Church of Green Mountain Antibodies in Burlington, Vermont in exchange for 2.0 mg of human, monomeric vitronectin antigen. The antibody was purified by gel filtration and ion exchange chromatography from murine ascites. The purity of the monoclonal antibody sample was determined by 10% SDS-PAGE. Crystal Screen™, Index™, and Low Ionic Strength™ protein crystal screens were purchased from Hampton Research. Both the ImmunoPure Fab Preparation Kit™ and the ImmunoPure F(ab')<sub>2</sub> Preparation Kit™ were purchased from Pierce Biotechnology. Plastic microtiter plates (Immunolon) were a product of Corning.

**Determining the Titer of GMA<sub>900</sub> Monoclonal Antibody via ELISA:** Vitronectin was purified from human plasma by a modification of the original protocol of Dahlback and Podack (Dahlback, *et al.*, 1985). A microtiter plate was coated with a 5 µg/ml vitronectin solution in 50 mM sodium carbonate (NaCO<sub>3</sub>), pH 8.5 as the coating buffer.



100  $\mu$ l of the vitronectin/coating buffer solution was added to each well. The microtiter plate was covered tightly with parafilm and held at room temperature for 4 hours.

The solution was emptied from the wells by shaking the microtiter plate into the sink and subsequently blotted dry on paper towels. The microtiter wells were then washed 3 times with 1X TBS, pH 7.4 and blotted dry between each rinse. Each well was then filled with 200  $\mu$ l of a 2% BSA blocking solution in TBS and set at room temperature to block for one hour. After blocking with 2% BSA, the microtiter plate was washed 3 times as described earlier. A serial dilution of monoclonal antibody (mAB) GMA<sub>900</sub> was set up. 100  $\mu$ l TBS with 0.2% BSA was pipetted into all wells in row one. 50  $\mu$ l TBS containing 0.2% BSA was pipetted into all wells in 3 through 12. The mAB was diluted to a concentration of 10  $\mu$ g/ml in TBS containing 0.2% BSA, and 100  $\mu$ l of this antibody solution was added to wells A through H in row 2. 50  $\mu$ l were removed from all of the wells in row 2 and subsequently mixed with the TBS buffer in row 3. In the same fashion, the monoclonal antibody solution was serially diluted through row 12. After 50  $\mu$ l of antibody was mixed from row 11 with the buffer in row 12, a final 50  $\mu$ l volume was removed from all wells in row 12 and discarded. The serially diluted monoclonal antibody was allowed to sit for one hour at room temperature to facilitate mAB binding to the vitronectin antigen.

The microtiter plate was again washed with TBS as previously described. An anti-mouse peroxidase-linked secondary antibody (Vector Laboratories) was diluted 1:1000 in TBS containing 0.2% BSA. 100  $\mu$ l of the diluted secondary antibody was pipetted into all wells. Again, the microtiter plate was allowed to sit for one hour at room



temperature to facilitate the binding of the secondary antibody to the primary monoclonal antibody. The plate was rinsed with TBS as described previously, and developing solution was made fresh by combining 100 ml of a 50 mM sodium citrate buffer, pH 5.5 with 20 mg of 2,2'-azino-bis(3-ethylbenzyl-thiazoline-6-sulfonic acid) diammonium salt (ABTS), and 50  $\mu$ l of a 30% hydrogen peroxide solution. 100  $\mu$ l of developing solution was pipetted into each well. The plate was allowed to develop in a Wallace 100™ microtiter plate reader for 30 minutes at room temperature. The plate was read with the wavelength set at 405 nm. Absorbance was measured every 5 minutes for 30 minutes to ensure readings were obtained within the linear range of the instrument. As shown in figure 3-3, the titer of the GMA<sub>900</sub> monoclonal antibody was determined to be approximately 1-5  $\mu$ g/ml.

***Preparation and Purification of Fab Fragments:*** The GMA<sub>900</sub> mAB was dialyzed extensively against a 20 mM sodium phosphate/10 mM EDTA buffer at pH 7.0, and concentrated to approximately 5 mg/ml. 0.5 ml of the mAB sample was added to 0.5 ml of digestion buffer (42 mg cysteine•HCl dissolved in 12 ml of the Phosphate Buffer, pH 10). Immobilized papain was equilibrated by adding 0.5 ml of the 50% immobilized papain (0.25 ml of immobilized papain) to a glass test tube, and 4.0 ml of digestion buffer were added. The papain was separated from the buffer using a serum separator tube, and the immobilized papain was resuspended in 0.5 ml of digestion buffer. 1.0 ml of mAB sample was added to the tube containing the immobilized papain and was incubated for 5 hours at 37°C while maintaining constant mixing at high speed. The solubilized Fab and Fc fragments and undigested IgG were recovered from the immobilized papain gel using a serum separator tube described above. The crude digest



|   | 1     | 2     | 3     | 4     | 5     | 6     | 7     | 8     | 9     | 10    | 11    |
|---|-------|-------|-------|-------|-------|-------|-------|-------|-------|-------|-------|
| A | 0.053 | 0.252 | 0.256 | 0.218 | 0.252 | 0.245 | 0.207 | 0.171 | 0.146 | 0.111 | 0.088 |
| B | 0.056 | 0.267 | 0.262 | 0.25  | 0.259 | 0.232 | 0.214 | 0.179 | 0.145 | 0.117 | 0.088 |
| C | 0.056 | 0.281 | 0.285 | 0.244 | 0.264 | 0.236 | 0.214 | 0.179 | 0.147 | 0.112 | 0.087 |
| D | 0.055 | 0.271 | 0.27  | 0.236 | 0.255 | 0.246 | 0.213 | 0.181 | 0.146 | 0.111 | 0.087 |
| E | 0.055 | 0.276 | 0.272 | 0.23  | 0.262 | 0.236 | 0.222 | 0.182 | 0.147 | 0.114 | 0.088 |
| F | 0.056 | 0.281 | 0.272 | 0.246 | 0.263 | 0.245 | 0.218 | 0.183 | 0.147 | 0.113 | 0.088 |
| G | 0.054 | 0.282 | 0.281 | 0.254 | 0.254 | 0.245 | 0.214 | 0.181 | 0.147 | 0.12  | 0.095 |
| H | 0.054 | 0.286 | 0.287 | 0.258 | 0.274 | 0.244 | 0.22  | 0.181 | 0.149 | 0.121 | 0.093 |

**Fig. 3-4:** Direct ELISA to measure the titer of GMA<sub>900</sub> Anti-Vitronectin Monoclonal Antibody. Titer determined to be approximately 1-5  $\mu$ g/ml.



was collected in a clean tube. For maximum recovery of fragments, the immobilized papain was washed with 1.5 ml of ImmunoPure® IgG Binding Buffer, and the wash was combined with the crude digest to give a 3.0 ml sample. The Fab fragments were initially purified using affinity chromatography with an AffinityPak™ protein A column as the initial purification step followed by gel filtration chromatography using an 18 ml column packed with Sephacryl S-100™ High Resolution Resin.

***Did the Proteolytic Fragments Retain Antigen Binding Property?*** Proteolytic cleavage of IgG molecules has been found to occasionally produce Fab fragments that, while still structurally intact, do not retain their antigen binding properties. Because the function of IgG fragment-based scaffold for protein crystallization relies entirely on the Fab fragments' ability to bind its antigen tightly, fragments that lose their antigen binding ability following proteolysis will never facilitate the crystallization of a host protein. Thus, it is crucial to assay the monoclonal antibody fragments for antigen binding potential.

The vitronectin binding potential of the purified Fab fragments will be assayed by gel filtration HPLC using a Phenomenex BioSep-SEC-S2000™ column. Vitronectin will be mixed with purified monoclonal Fab fragments in differing molar ratios. Binding will be assayed based on protein sample elution times. After characterizing the elution times of protein standards covering the linear molecular weight range, both vitronectin and Fab will be injected separately, and the characteristic elution times of each sample will be recorded.



By injecting a sample containing vitronectin and Fab fragments, the degree of binding can be quantitatively determined. If the Fab fragments bind the vitronectin, a new elution-time peak representing the vitronectin-Fab complex will appear. By integrating the area under the elution-time peaks, the extent of binding can be determined by assessing the integrated elution peak ratios. If the Fab fragments do not retain their antigen binding property, there will be two elution-time peaks on the chromatograph representing uncomplexed Fab and vitronectin identical to the elution times determined previously for each species independently. In contrast, if 100% of both protein samples participate in complex formation, one elution peak characteristic of a higher molecular weight species of approximately 120 kDa (72 for vitronectin + 50 for Fab fragments) will be observed.

#### ***Determination of Vitronectin-IgG Fragment Stoichiometry and Optimization of Complex Formation***

If it is determined that the Fab fragments did in fact retain their antigen binding property, determination of the vitronectin-IgG Fragment binding stoichiometry and optimization of complex formation will be determined using analytical ultracentrifugation sedimentation equilibrium experiments carried out at 277 K on a Beckmann Optima XL-A instrument. 100 ml aliquots will be centrifuged at 50,000 RPM. Radial scans of the absorbance at 280 nm will be taken at different time intervals. The distribution of a single, homogeneous species within the ultracentrifuge cell at equilibrium is given by,

$$c_r = c_m \exp(\sigma) + \text{base} \quad (\text{Eq. 1})$$

$$\sigma = M(1 - \bar{v} \rho) \omega^2 (r^2 - r_m^2) / 2RT \quad (\text{Eq. 2})$$



in which  $c_r$  and  $c_m$  are the concentrations of the protein at radial position,  $r$ , and at a reference position (*i.e.* the meniscus), respectively, within the cell.  $M$  is the protein molecular weight,  $\bar{v}$  is the partial specific volume,  $\omega$  is the angular velocity,  $\rho$  is solvent density,  $r$  is the distance in cm from the center of the rotor,  $r_m$  is the radial position in cm of the reference from the center of rotation,  $R$  is the gas constant, and  $T$  is absolute temperature. The "base" term is a constant that corrects for non-sedimenting baseline absorbance (or fringes measured). The partial specific volume will be calculated from the composition of vitronectin and Fab, and its use for analysis of equilibrium centrifugation data will yield reliable molecular weights for the isolated monomeric proteins using Equation 1. The calculation of partial specific volume for vitronectin from its amino acid and oligosaccharide composition was previously reported and used in published ultracentrifugation analyses on vitronectin (Zhuang, *et al.*, 1996). For an associating system, at chemical and sedimentation equilibrium, in which, for example,  $A + B \rightleftharpoons AB$ , the sedimentation behavior of each individual macromolecular species, A, B, and AB, is also given by the exponential distribution described above (Hensley 1996). The total macromolecule concentration at any radial position is equal to the sum of all of the individual species, *i.e.*  $A + B + AB$ , and the overall distribution of macromolecules is given by the sum of the individual contributions for each species, A, B, and AB, as,

$$C_r = c_{m,A} \cdot \exp(\sigma_A) + c_{m,B} \cdot \exp(\sigma_B) + c_{m,AB} \cdot \exp(\sigma_{AB}) + \text{base} \quad (\text{Eq. 3})$$

According to the law of mass action,  $c_{AB}$  equals  $c_A \cdot c_B / K_{AB}$ , in which  $K_{AB}$  equals the equilibrium constant for the associating system. Thus Equation 3 shows that



sedimentation and chemical equilibria exist at all radial positions in the ultracentrifuge cell. Equation 3 may be generalized in the form of Equation 4, for species  $i$ .

$$C_r = \sum c_{m,i} \cdot \exp(\sigma_i) + \text{base} \quad (\text{Eq. 4})$$

It should be noted that this equation is applicable to any mixture of sedimenting species. The monomer molecular weights for vitronectin and Fab determined using Equation 1, as described above, will be used in Equation 4 to calculate the molecular weight of the complex. Data were analyzed using nonlinear least squares methods, as described by Brooks, *et al.*, 1994 using IGOR (Wavemetrics, Lake Oswego, OR).

**Crystal Screening:** Vitronectin from a precipitated ammonium sulfate slurry and Fab thawed in an ice bucket will be dialyzed extensively against a 0.02 M Tris, pH 7.4 at 4°C. The complex will be incubated for one hour using the molar ratios determined from optimization experiments. Purity of the vitronectin-Fab sample will be analyzed using SDS-PAGE. The vitronectin-Fab sample will be concentrated to approximately 10 mg/ml using a .5 Ultrafree™ 30,000 MWCO centrifugal concentration device and prior to screening, any amorphous material present in the sample will be removed by centrifugation at 10,000 RPM at 4°C.

Screening of crystallization conditions for the vitronectin-Fab complex will be performed using the hanging-drop vapor diffusion method using two approaches. The first will be the standard screening method (Jancarik, & Kim, 1991; Cudney, *et al.*, 1994) using Crystal Screen™ and Index™ kits. The second approach will employ Low Ionic Strength™ crystal screen from Hampton Research. The protocol has been shown to be an effective screen for determining the preliminary crystallization conditions of intact



monoclonal antibodies, monoclonal antibody fragments, and other soluble proteins (Harris, *et al.*, 1995). An extremely broad range of pH 2.0 to 12.0 is sampled. At low ionic strength the effects of pH and temperature upon protein solubility are augmented, thus this screen allows one to critically evaluate the effects of solubility in crystallization.

### Chapter Three

#### EXPRESSION OF RECOMBINANT, FULL-LENGTH, NATIVE, MONOMERIC VITRONECTIN IN BABY HAMSTERT KIDNEY CELLS (BHK cells)

**Rationale:** Vitronectin research is technically demanding from a laboratory standpoint. Preparations of native vitronectin from pooled human plasma takes approximately 2 weeks, and the protein yield is only between 5-30 mg. As a result, one vitronectin preparation generates only enough protein for a limited number of experiments, for crystallization studies require milligram quantities of the protein. Thus, the lack of an expression system for generating recombinant, full-length vitronectin has impeded many facets of vitronectin research, namely structural studies.

The power of site-directed mutagenesis (SDM) is demonstrated by its utility in nearly all facets of protein research. The ability to use this technique in the study of a particular protein relies on the capability to recombinantly express it. Such recombinant



expression becomes a significant tool for protein manipulation. With vitronectin crystallization in particular, SDM would allow the expression of a deglycosylated mutant that has not been able to be generated via standard enzyme-based chemistry. Additionally, vitronectin exists natively in serum in two forms, a double chain form and a single chain form that results from post-translational, proteolytic cleavage. Because crystallization is dependent upon sample homogeneity, SDM could allow the expression

### **Chapter Three**

## **EXPRESSION OF RECOMBINANT, FULL-LENGTH, NATIVE, MONOMERIC VITRONECTIN IN BABY HAMSTERT KIDNEY CELLS (BHK cells)**

**Rationale:** Vitronectin research is technically demanding from a laboratory standpoint. Preparations of native vitronectin from pooled human plasma takes approximately 2 weeks, and the protein yield is only between 5-30 mg. As a result, one vitronectin preparation generates only enough protein for a limited number of experiments, for crystallization studies require milligram quantities of the protein. Thus, the lack of an expression system for generating recombinant, full-length vitronectin has impeded many facets of vitronectin research, namely structural studies

The power of site-directed mutagenesis (SDM) is demonstrated by its utility in nearly all facets of protein research. The ability to use this technique in the study of a particular protein relies on the capability to recombinantly express it. Such recombinant



expression becomes a significant tool for protein manipulation. With vitronectin crystallization in particular, SDM would allow the expression of a deglycosylated mutant that has not been able to be generated via standard enzyme-based chemistry. Additionally, vitronectin exists natively in serum in two forms, a double chain form and a single chain form that results from post-translational, proteolytic cleavage. Because crystallization is dependent upon sample homogeneity, SDM could allow the expression and therefore purification of a one-chain, homogenous vitronectin sample better suited for crystal screening. With these facts in mind, I have devoted focus into the successful recombinant expression of vitronectin. Success in this endeavor would not only decrease the laborious, low-yield process of vitronectin isolation from human serum, but it would also allow SDM to be employed in crystallization studies and augment the promise of my research.

Successful expression of mammalian serum proteins such as factor XIII, transferring, and antithrombin III has been performed using the pNUT/BHK expression system (Fan, *et al.* 1993). In light of this success, this expression system will be used in an attempt to express full-length vitronectin.

## **Experimental Procedures**

**Materials:** An *Escherichia coli* M1190 strain housing the vitronectin gene was prepared by Dr. Cynthia Peterson. Oligonucleotide primers for PCR were purchased from Oligos Etc®. Plasmid DNA isolation was performed using a MiniPrep™ Kit from Promega. PCR and transformation experiments were performed using the TA Cloning Kit from Invitrogen®.



**Engineering NotI Restriction Sites into the Vitronectin Gene:** The plasmid from an *Escherichia coli* M1190 strain housing the 1.7 k.b. vitronectin gene in pUC18 (fig. 4-1) was isolated from a 50 ml cell culture. Oligonucleotide primers (fig 4-2) were designed so as to engineer a NotI restriction (GCGGCCGC) site on the 5' and 3' termini of the gene. The vitronectin gene was PCR amplified for 30 cycles using the NotI-tagged primers. The 50 µl PCR reaction volume consisted of 1.0 µl pUC18-vitronectin plasmid template, 5 µl 10X PCR buffer (60 mM Tris-HCl, pH 7.5/60 mM MgCl<sub>2</sub>/50 mM NaCl/1 mg/ml bovine serum albumin/70 mM β-mercaptoethanol/1 mM ATP /20 mM dithiothreitol /10 mM spermidine), .5 µl of 50mM dNTPs (12.5 mM dATP/12.5 mM dCTP /12.5 mM dGTP /12.5 mM dTTP, adjusted to pH 8.0), 5 µl primer, 32.5 µl sterile water, and 1.0 µl *Xtaq*<sup>TM</sup> DNA polymerase (Innis, *et al.*,1990Z). Amplification was assayed using agarose gel electrophoresis with ethidium bromide under a U.V. lamp (fig. 3-3).

The resulting PCR product will be cloned into a pCR2.1<sup>TM</sup> (Invitrogen) shuttle vector, which will be used to transform the plasmid into competent cells. The sequence of the gene will be sequenced in order to verify the directionality of my insert as well as verify PCR integrity. The NotI-tagged vitronectin gene will be cloned into pNUT, which harbors an inducible, mammalian promoter, and the pNUT vector will be used to express vitronectin recombinantly in BHK cells.



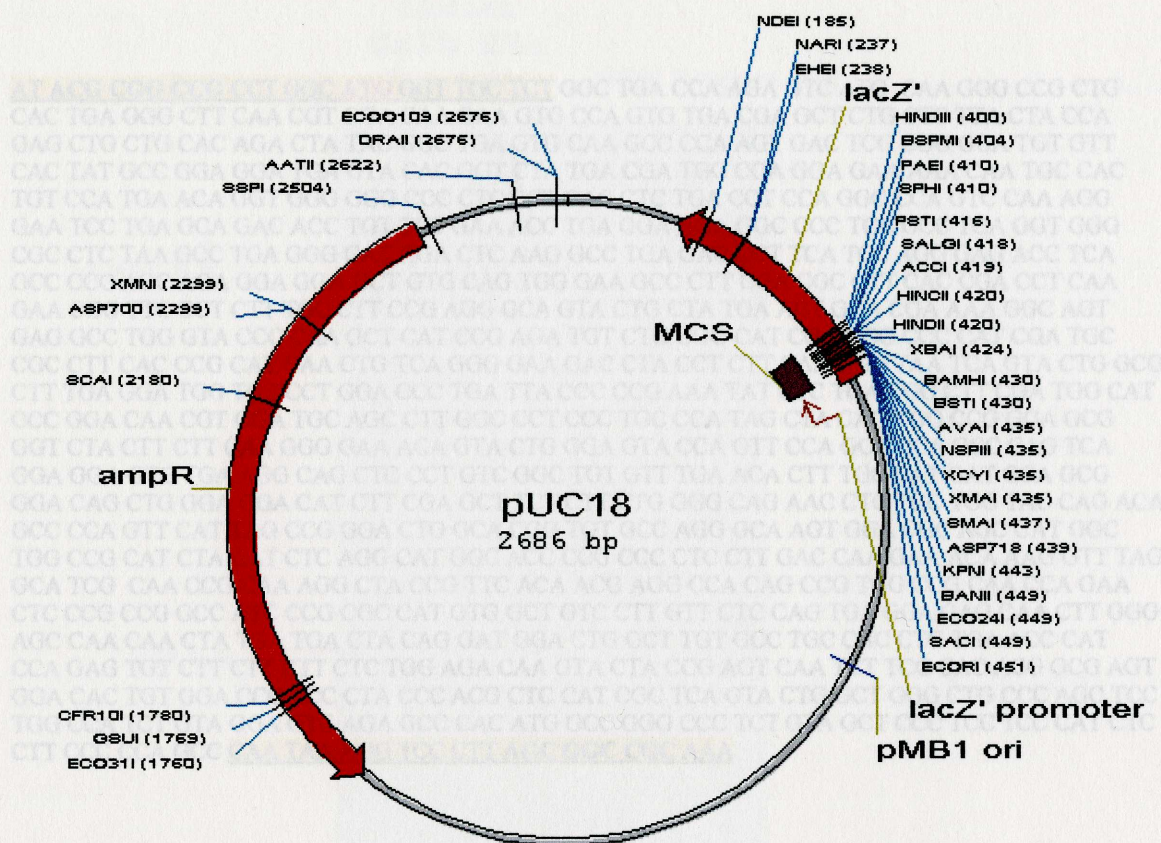


Figure 4-2. The 1502 base sequence of the **lacZ'** gene. The sequences highlighted in yellow constitute the oligonucleotide primer sequences used to mutate in the **NdeI** restriction enzyme sites. Bases shown in blue are the **NdeI** restriction sequences. The red sequence

**Fig. 4-1: pUC18 Restriction Map.** The vitronectin gene was cloned into pUC18 using the **EcoRI** restriction site.



Lambda  
BstXI DNA

**AT ACG CGG CCG CCT GGC ATG GGT TGC TCT** GGC TGA CCA AGA GTC ATG CAA GGG CCG CTG  
CAC TGA GGG CTT CAA CGT GGA CAA GAA GTG CCA GTG TGA CGA GCT CTG CTC TTA CTA CCA  
GAG CTG CTG CAC AGA CTA TAC GGC TGA GTG CAA GCC CCA AGT GAC TCG CGG GGA TGT GTT  
CAC TAT GCC GGA GGA TGA GTA CAC GGT CTA TGA CGA TGG CGA GGA GAA AAA CAA TGC CAC  
TGT CCA TGA ACA GGT GGG GGG CCC CTC CCT GAC CTC TGA CCT CCA GGC CCA GTC CAA AGG  
GAA TCC TGA GCA GAC ACC TGT TCT GAA ACC TGA GGA AGA GGC CCC TGC GCC TGA GGT GGG  
CGC CTC TAA GCC TGA GGG GAT AGA CTC AAG GCC TGA GAC CCT TCA TCC AGG GAG ACC TCA  
GCC CCC AGC AGA GGA GGA GCT GTG CAG TGG GAA GCC CTT CGA CGC CTT CAC CGA CCT CAA  
GAA CGG TTC CCT CTT TGC CTT CCG AGG GCA GTA CTG CTA TGA ACT GGA CGA AAA GGC AGT  
GAG GCC TGG GTA CCC CAA GCT CAT CCG AGA TGT CTG GGG CAT CGA GGG CCC CAT CGA TGC  
CGC CTT CAC CCG CAT CAA CTG TCA GGG GAA GAC CTA CCT CTT CAA GGG TAA TCA GTA CTG GCG  
CTT TGA GGA TGG TGT CCT GGA CCC TGA TTA CCC CCG AAA TAT CTC TGA CGG CTT CGA TGG CAT  
CCC GGA CAA CGT GGA TGC AGC CTT GGC CCT CCC TGC CCA TAG CTA CAG TGG CCG GGA GCG  
GGT CTA CTT CTT CAA GGG GAA ACA GTA CTG GGA GTA CCA GTT CCA GCA CCA GCC CAG TCA  
GGA GGA GTG TGA AGG CAG CTC CCT GTC GGC TGT GTT TGA ACA CTT TGC CAT GAT GCA GCG  
GGA CAG CTG GGA GGA CAT CTT CGA GCT TCT CTT CTG GGG CAG AAC CTC TGC TGG TAC CAG ACA  
GCC CCA GTT CAT TAG CCG GGA CTG GCA CGG TGT GCC AGG GCA AGT GGA CGC AGC CAT GGC  
TGG CCG CAT CTA CAT CTC AGG CAT GGC ACC CCG CCC CTC CTT GAC CAA GAA ACA AAG GTT TAG  
GCA TCG CAA CCG CAA AGG CTA CCG TTC ACA ACG AGG CCA CAG CCG TGG CCG CAA CCA GAA  
CTC CCG CCG GCC ATC CCG CGC CAT GTG GCT GTC CTT GTT CTC CAG TGA GGA GAG CAA CTT GGG  
AGC CAA CAA CTA TGA TGA CTA CAG GAT GGA CTG GCT TGT GCC TGC CAC CTG TGA ACC CAT  
CCA GAG TGT CTT CTT CTT CTC TGG AGA CAA GTA CTA CCG AGT CAA TCT TCG CAC ACG GCG AGT  
GGA CAC TGT GGA CCC TCC CTA CCC ACG CTC CAT CGC TCA GTA CTG GCT GGG CTG CCC AGC TCC  
TGG CCA TCT GTA GGA GTC AGA GCC CAC ATG GCC GGG CCC TCT GTA GCT CCC TCC TCC CAT CTC  
CTT CCC CCA GCC **CAA TAA AGG TCC CTT AGC GGC CGC AAA**

**Figure 4-2:** The 1502 base sequence of the . The sequences highlighted in yellow constitute the oligonucleotide primer sequences used to mutate in the NotI restriction enzyme sites. Bases shown in blue are the NotI restriction sequences. The red sequence denotes the start codon initiating the open reading frame of the human vitronectin gene.

engineered 5' and 3' NotI restriction sites



## REFERENCES

Barnes, D. W., Reing, J. E., and Amos, B. (1985) *J. Biol. Chem.* 260(16), 9117-22. "Heparin-binding properties of vitronectin spreading factor."

Bhattacharya, S., Fu, C., Bhattacharya, S., and Bhattacharya, S. (1995) *J. Biol. Chem.* 270 (28), 16781-16787. "Sialin, a member of the integrin family, mediates enhanced tyrosine phosphorylation of vitronectin in bovine pulmonary artery endothelial cells."

Fan, B. C., and Gettings, P. (1993) *K. Biol. Chem.* 268(33), 24838-46. "Alteration of vitronectin-induced tyrosine phosphorylation by treatment with urea."

Bittorf, S. V., Williams, J. L., and Williams, J. L. (1990) *J. Biol. Chem.* 265(1), 1-10. "Crystallization mechanisms in solution."

Boistelle, R., and Astier, J. (1990) *J. Biol. Chem.* 265(1), 1-10. "Crystallization mechanisms in solution."

Braden, B. C., Souchon, R. J., and Poljak, R. J. (1994) *J. Mol. Biol.* 244(1), 1-10. "The free and the antigenic epitopes of vitronectin are located in the same region of the molecule."

Buckley, M. F., Lovelace, J. E., and Ghosh, J. W. (1990) *J. Biol. Chem.* 265(1), 1-10. "cDNA cloning of the human molecule, amino acid sequence, and chromosomal location."

Chain, D., Kore-Grodzicki, B., Kreizman, T., and Shaltiel, S. (1990) *FEBS Lett.* 269, 221-225. "The phosphorylation of the two-chain form of vitronectin by protein kinase A is heparin-dependent."

Chain, D., Kreizman, T., Shapira, H., and Shaltiel, S. (1990) *FEBS Lett.* 269, 221-225. "Plasmin cleavage of vitronectin: identification of the site and consequent attenuation in binding plasminogen activator inhibitor-1."

Chain, D., Kreizman, T., Shapira, H., and Shaltiel, S. (1991) *FEBS Lett.* 285, 251-256. "Plasmin cleavage of vitronectin: identification of the site and consequent attenuation in binding plasminogen activator-inhibitor-1."

Chain, D., Kreizman, T., Shapira, H., and Shaltiel, S. (1991) *FEBS Lett.* 285, 251-256. "Plasmin cleavage of vitronectin: identification of the site and consequent attenuation in binding plasminogen activator-inhibitor-1."

**Lambda  
BstEII DNA  
Standards**

**PCR Product**

8.454 k.b.

1.929 k.b.

1.7 k.b.

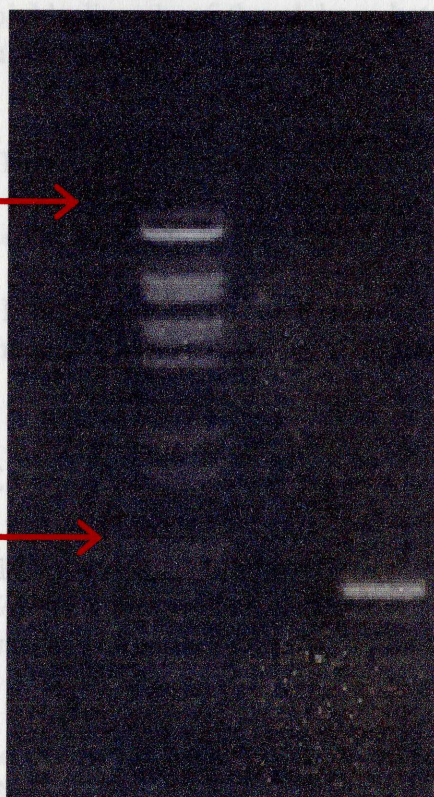


**Figure 4-3:** 1% Agarose Gel PCR Product Analysis: the 1.7 k.b. vitronectin gene with engineered 5' and 3' NotI restriction sites



## REFERENCES

- Barnes, D. W., Reing, J. E., and Amos, B. (1985) *J. Biol. Chem.* **260**(16), 9117-22. "Heparin-binding properties of human serum spreading factor."
- Bhattacharya, S., Fu, C., Bhattacharya, J., and Greenberg, S. (1995) *J. Biol. Chem.* **270**(28), 16781-16787. "Soluble ligands of the alpha v beta 3 integrin mediate enhanced tyrosine phosphorylation of multiple proteins in adherent bovine pulmonary artery endothelial cells."
- Fan, B., Crewst, B. C., Turko, I. V., Choay, J., Zettlmei, G., and Gettins, P. (1993) *K. Biol. Chem.* **268**(23), 17588-17596. "Heterogeneity of Recombinant Human Antithrombin III Expressed in Baby Hamster Kidney Cells."
- Bittorf, S. V., Williams, E. C., and Mosher, D. F. (1993) *J. Biol. Chem.* **268**(33), 24838-46. "Alteration of vitronectin. Characterization of changes induced by treatment with urea."
- Boistelle, R. and Astier, J. P. (1988) *J. of Cryst. Growth.* **90**, 14-30. "Crystallization mechanisms in solution."
- Braden, B.C., Souchon, H., Eisele, J.L., Bentley, G. A., Bhat, T. N., Navaza, J., and Poljak, R. J. (1994) *J. Mol. Biol.* Nov 4; **243**(4), 767-81. "Three-dimensional structures of the free and the antigen-complexed Fab from monoclonal anti-lysozyme antibody D44.1."
- Buckley, M. F., Loveland, K. A., Mckinsty, W. J., Garson, O. M., and Ghodasing, J. W. (1990) *J. Biol. Chem.* **265**, 17506-17511. "Plasma cell membrane glycoprotein PC-1. cDNA cloning of the human molecule, amino acid sequence, and chromosomal location."
- Cardin, A. D., and Weintraub, H. J. R. (1989) *Arteriosclerosis* **9**, 21-31. "Molecular modeling of protein-glycosaminoglycan interactions."
- Chain, D., Korc-Grodzicki, B., Kreizman, T., and Shaltiel, S. (1990) *FEBS Lett.* **269**, 221-225. "The phosphorylation of the two-chain form of vitronectin by protein kinase A is heparin-dependent."
- Chain, D., Kreizman, T., Shapira, H., and Shaltiel, S. (1990) *FEBS Lett.* **269**, 221-225. "Plasmin cleavage of vitronectin: identification of the site and consequent attenuation in binding plasminogen activator inhibitor-1."
- Chain, D., Kreizman, T., Shapira, H., and Shaltiel, S. (1991) *FEBS Lett.* **285**, 251-256. "Plasmin cleavage of vitronectin: identification of the site and consequent attenuation in binding plasminogen activator-inhibitor-1."



- Chang, C. Y., Jeffrey, P. D., Bajorath, J., Hellstrom, I., Hellstrom, K. E. and Sheriff, S. (1994). *J. Mol. Biol.* **235**, 372-376.
- Chang, C. Y., Whitaker, P. B., Tabernero, L., Einspahr, H., Workman, L., Benjamin, D. C. and Sheriff, S. (1994). *J. Mol. Biol.* **239**, 154-157.
- Cherny, R. C., Honan, M. A., and Thiagarajan, P. (1993) *J. Biol. Chem.* **268** (13), 9725-9. "Site-directed mutagenesis of the arginine-glycine-aspartic acid in vitronectin abolishes cell adhesion."
- Conlan, M. G., Tomasini, B. R., Schultz, R. L., and Mosher, D. F. (1988) *Blood* **72**, 185-190. "plasma vitronectin polymorphism in normal subjects and patients with disseminated intravascular coagulation."
- Cudney, R., Patel, S., Weisgraber, K., Newhouse, Y. and McPherson, A. (1994). *Acta Cryst.* **D50**, 414-423.
- Dahlback, K., Wulf, H. C., and Dahlback, B. (1993) *J. Invest Dermatol.* **100** (2), 166-70. "Vitronectin in mouse skin: immunohistochemical demonstration of."
- Dahlback, B., and Podack, E. R. (1985) *Biochem.* **24**, 2368-2374. "Characterization of human S protein, an inhibitor of the membrane attack complex of complement. Demonstration of a free reactive thiol group."
- de Boer, H. C., Preissner, K. T., Bouma, B. N., and de Groot, P. G. (1992) *J. Biol. Chem.* **267**(4), 2264-8. "Binding of vitronectin-thrombin-antithrombin III complex to human endothelial cells is mediated by the heparin binding site of vitronectin."
- de Boer, H. C., de Groot, P. G., Bouma, B. N., and Preissner, K. T. (1993) *J Biol Chem* **268** (2), 1279-83. "Ternary vitronectin-thrombin-antithrombin III complexes in human plasma. Detection and mode of association"
- Declercq, P.J., DeMol, M., Alessi, M.-C., Baudner, S., Paques, E.-P., Preissner, K. T., Muller-Berghaus, G., and Collen, D. (1988) *J. Biol. Chem.* **263**, 15454-15461. "Purification and characterization of a plasminogen activator inhibitor 1 binding protein from human plasma. Identification as a multimeric form of S protein (vitronectin)."
- Deng, G., Curriden, S. A., Wang, S., Rosenberg, S., and Loskutoff, D. J. (1996) *J. Cell Biol.* **134**(6), 1563-71. "Is plasminogen activator inhibitor-1 the molecular switch that governs urokinase receptor-mediated cell adhesion and release?"
- Deng, G., Curriden, S. A., Hu, G., Czekay, R. P., and Loskutoff, D. J. (2001) *J Cell Physiol* **189**(1), 23-33. "Plasminogen activator inhibitor-1 regulates cell adhesion by binding to the somatomedin B domain of vitronectin"



Drenth, J. and Haas, C. J. (1992) *Cryst. Growth* **122**,107-109. "Protein crystals and their stability."

Eitzman, D. T., Westrick, R. J., Nabel, E. G., and Ginsburg, D. (2000) *Blood* **95**(2), 577-80. "Plasminogen activator inhibitor-1 and vitronectin promote vascular thrombosis in mice"

Faber, H. R., Groom, C. R., Baker, H. M., Morgan, W. T., Smith, A., and Baker, E. N. (1995) *Structure* **3**(6), 551-9. "1.8 Å crystal structure of the C-terminal domain of rabbit serum haemopexin"

Fay, W. P., Parker, A. C., Ansari, M. N., Zheng, X., and Ginsburg, D. (1999) *Blood* **93**(6), 1825-30. "Vitronectin inhibits the thrombotic response to arterial injury in mice"

Feher, G. and Kam, Z. (1985) *Meth. Enz.* **114**, 77-111,. "Nucleation and growth of protein crystals: general principles and assays."

Fischmann, T. O., Bentley, G. A., Bhat, T. N., Boulot, G., Mariuzza, R. A., Phillips, S. E., Tello, D. & Poljak, R. J. (1991). *J. Biol. Chem.* **266**, 12915-12920.

Geb, C., Hayman, E. G., Engvall, E., and Ruoslahti, E. (1986) *J. Biol. Chem.* **261**, 16698-16703. "Interaction of vitronectin with collagen."

Gechtman, Z., Sharma, R., Kreizman, T., Fridkin, M., and Shaltiel, S. (1993) *FEBS Lett.* **315**(3), 293-7. "Synthetic peptides derived from the sequence around the plasmin cleavage site in vitronectin. Use in mapping the PAI-1 binding site."

Gechtman, Z., and Shaltiel, S. (1997) *Eur. J. Biochem.* **243** (1-2), 493-501. "Phosphorylation of vitronectin on Ser 362 by protein kinase C attenuates its cleavage by plasmin."

Gechtman, Z., Belleli, A., Lechpammer, S., and Shaltiel, S. (1997) *Biochem J* **325**(Pt 2), 339-49. "The cluster of basic amino acids in vitronectin contributes to its binding of plasminogen activator inhibitor-1: evidence from thrombin-, elastase- and plasmin-cleaved vitronectins and anti-peptide antibodies"

Germer, M., Kanse, S. M., Kirkegaard, T., Kjoller, L., Felding-Habermann, B., Goodman, S., and Preissner, K. T. (1998) *Eur J Biochem* **253**(3), 669-74. "Kinetic analysis of integrin-dependent cell adhesion on vitronectin-- the inhibitory potential of plasminogen activator inhibitor-1 and RGD peptides"

Gibson, A. D., Lamerdin, J. A., Zhuang, P., Baburaj, K., Serpersu, E. H., and Peterson, C. B. (1999) *J Biol Chem* **274**(10), 6432-42. "Orientation of heparin-binding sites in native vitronectin. Analyses of ligand binding to the primary glycosaminoglycan-binding site indicate that putative secondary sites are not functional"



Goding, J.W. (1978) *J. Immunol. Meth.* **20**, 241-253. "Use of staphylococcal protein A as an immunological reagent."

Goding, J. (1983) *Monoclonal Antibodies: Principles and practice*. Academic Press Inc. London, 118-122.

Gohlke, U., Gomis-Ruth, F. X., Crabbe, T., Murphy, G., Docherty, A. J. P., and Bode, W.-P. (1996) *FEBS Lett.* **373**, 126-130. "The C-terminal (haemopexin-like) domain structure of human gelatinase-A (MMP2): structural implications for its function."

Gomis-Ruth, F. X., Gohlke, M., Betz, M., Knauper, V., Murphy, G., Lopez-Otin, C., and Bode, W. (1996) *J. Mol. Biol.* **264**, 556-566. "The helping hand of collagenase-3 (MMP-13): 2.7 Å crystal structure of its C-terminal haemopexin-like domain."

Harris, Lisa J., Skaletsky, E., and McPherson, A. (1995) *Proteins: Structure, Function, and Genetics*, **23**, 285-289. "Crystallization of intact monoclonal antibodies."

Hayashi, M., Akama, T., Kono, I., and Kashiwagi, H. (1985) *J. Biochem. (Tokyo)* **98**(4), 1135-8. "Activation of vitronectin (serum spreading factor) binding of heparin by denaturing agents."

Hayman, E. G., Pierschbacher, M. D., Ohgren, Y., and Ruoslahti, E. (1983) *Proc. Natl. Acad. Sci.* **80**, 4003-4007. "Serum spreading factor is present at the cell surface and in tissues."

Hayman, E. G., Pierschbacher, M. D., Suzuki, S., and Ruoslahti, E. (1985) *Exp. Cell Res.* **160**, 245-258. "Vitronectin—a major cell attachment-promoting protein in fetal bovine serum."

Haynes, M. R., Stura, E. A., Hilvert, D., and Wilson, I. A. (1994) *Science*, **263**, 646-652.

Heckman, C. M., and Loskutoff, D. J. (1988) *Arch. Biochem. Biophys.* **262**, 199-210. "Kinetic analysis of the interactions between plasminogen activator inhibitor I and both urokinase and tissue plasminogen activator."

Holmes, R. (1967) *J. Cell Biol.* **32**, 297-308. "Preparation from human serum of an alpha-one protein which induces the immediate growth of unadapted cells *in vitro*."

Horton, M. A. (1997) *Int. J. Biochem. Cell Biol.* **29** (5), 721-725. "The alpha v beta 3 integrin "vitronectin receptor."

Huber, R., and Carrell, R. W. (1989) *Biochem.* **28**, 8951-8966. "Implications of the three-dimensional structure of alpha 1-antitrypsin for structure and function of serpins."



- Ill, C. R., and Ruoslahti, E. (1985) *J Biol Chem* **260**(29), 15610-5. "Association of thrombin-antithrombin III complex with vitronectin in serum"
- Imai, K., Shikata, H., and Okada, Y. (1995) *FEBS Lett.* **369**, 249-251. "Degradation of vitronectin by metalloproteinases-1, -2, -3, -7, and -9."
- Ishikawa, M., and Hayashi, M. (1992) *Biochim. Biophys. Acta* **1121**, 173-177. "Activation of the collagen-binding of endogenous serum vitronectin by heating, urea, and glycosaminoglycans."
- Ishikawa-Sakurai, M., and Hayashi, M. (1993) *Cell Struct. Funct.* **18** (4), 253-259. "Two collagen-binding domains of vitronectin."
- Izumi, M., Shimo-Oka, T., Morishita, N., Ii, I., and Hayashi, M. (1998) *Cell Struct. Funct.* **13**, 217-225. "Identification of the collagen-binding domain of vitronectin using monoclonal antibodies."
- Jancarik, J. & Kim, S.-H. (1991) *J. Appl. Cryst.* **24**, 409-411.
- Jenne, D., and Stanley, K. K. (1987) *Biochemistry* **26**(21), 6735-42. "Nucleotide sequence and organization of the human S-protein gene: repeating peptide motifs in the "pexin" family and a model for their evolution"
- Jenne, D., Hille, A., Stanley, K. K., and Huttner, W. B. (1989) *Eur. J. Biochem.* **185**, 391-395. "Sulfation of two tyrosine-residues in human complement S-protein (vitronectin)."
- Kambayashi, J. I., and Sakon, M. (1989) *Methods. Enzymol.* **169**, 422-454. "Calcium-dependent proteases and their inhibitors in human platelets."
- Kjoller, L., Kanse, S. M., Kirkegaard, T., Rodenburg, K. W., Ronne, E., Goodman, S. L., Preissner, K. T., Ossowski, L., and Andreasen, P. A. (1997) *Exp Cell Res* **232**(2), 420-9. "Plasminogen activator inhibitor-1 represses integrin- and vitronectin- mediated cell migration independently of its function as an inhibitor of plasminogen activation"
- Konstantinides, S., Schafer, K., Thinnies, T., and Loskutoff, D. J. (2001) *Circulation* **103**(4), 576-583. "Plasminogen Activator Inhibitor-1 and Its Cofactor Vitronectin Stabilize Arterial Thrombi After Vascular Injury in Mice"
- Korc-Grodzicki, B., Tauber-Finkelstein, M., Chain, D., and Shaltiel, S. (1998) *Biochem. Biophys. Res. Commun.* **157**, 1131-1138. "Vitronectin is phosphorylated by a cAMP-dependent protein kinase released by activation of human platelets with thrombin."



Korc-Grodzicki, B., Chain, D., Kreizman, T., and Shaltiel, S. (1990) *Anal. Biochem.* **188**, 288-294. "An enzymatic assay for vitronectin based on its selective phosphorylation by protein kinase A."

Kost, C., Stuber, W., Ehrlich, H. J., Pannekoek, H., and Preissner, K. T. (1992) *J. Biol. Chem.* **267**(17), 12098-105. "Mapping of binding sites for heparin, plasminogen activator inhibitor- 1, and plasminogen to vitronectin's heparin-binding region reveals a novel vitronectin-dependent feedback mechanism for the control of plasmin formation."

Kost, C., Stuber, W., Ehrlich, H. J., Pannekoek, H., and Preissner, K. T. (1992) *J. Biol. Chem.* **267**(17), 12098-105. "Mapping of binding sites for heparin, plasminogen activator inhibitor- 1, and plasminogen to vitronectin's heparin-binding region reveals a novel vitronectin-dependent feedback mechanism for the control of plasmin formation."

Kost, C., Benner, K., Stockmann, A., Linder, D., and Preissner, K. T. (1996) *Eur J Biochem* **236**(2), 682-8. "Limited plasmin proteolysis of vitronectin. Characterization of the adhesion protein as morpho-regulatory and angiostatin-binding factor"

Laver, W. G. (1990). *Methods*, **1**, 70-74.

Lawrence, D. A., Berkenpas, M. B., Palaniappan, S., and Ginsburg, D. (1994) *J Biol Chem* **269**(21), 15223-8. "Localization of vitronectin binding domain in plasminogen activator inhibitor-1."

Lawrence, D. A., Palaniappan, S., Stefansson, S., Olson, S. T., Francis-Chmura, A. M., Shore, J. D., and Ginsburg, D. (1997) *J. Biol. Chem.* **272**(12), 7676-80. "Characterization of the binding of different conformational forms of plasminogen activator inhibitor-1 to vitronectin. Implications for the regulation of pericellular proteolysis."

Liang, O. D., Rosenblatt, S., Chhatwal, G. S., and Preissner, K. T. (1997) *FEBS Lett.* **407** (2), 169-172. "Identification of novel heparin-binding domains of vitronectin."

Liu, J., Tse, A. G., Chang, H. C., Liu, J., Wang, J., Hussey, R. E., Chishti, Y., Rheinhold, B., Spoerl, R., Nathenson, S. G., Sacchettini, J. C. & Reinherz, E. L. (1996) *J. Biol. Chem.* **271**, 33639-33646.

Mage, M.G. (1980) *Meth., Enzymol.* **70**, 142-150. "Preparation of Fab fragments from IgGs of different animal species."

McGuire, E. A., Peacock, M. E., Inhorn, R. C., Siegel, N. R., and Tollefsen, D. M. (1988) *J. Biol. Chem.* **263**, 1942-1945. "Phosphorylation of vitronectin by a protein kinase in human plasma. Identification of a unique phosphorylation site in the heparin-binding domain."



Merberg, D. M., Fitz, L. J., Temple, P., Gianotti, J., Murtha, P., Fitzgerald, M., Scalreto, J., Kelleher, K., Preissner, K., Kriz, R., Jacobs, K., and Turner, K. (1993) in *Biology of Vitronectin and Their Receptors* (Preissner, K. T., Rosenblatt, S., Kost, C., Wegerhoff, J., and Mosher, D. F., eds), pp. 45-52, Elsevier, Amsterdam.

Milis, L., Morris, C. A., Sheehan, M. C., Charlesworth, J. A., and Pussell, B. A. (1993) *Clin. Exp. Immunol.* **92**(1), 114-9. "Vitronectin-mediated inhibition of complement: evidence for different binding sites for C5b-7 and C9."

Mimuro, J., Schleef, R. R., and Loskutoff, D. J. (1987) *Blood* **70**, 721-728. "Extracellular matrix of cultured bovine aortic endothelial cells contains functionally active type I plasminogen activator inhibitor."

Mimuro, J., and Loskutoff, D.J. (1989) *J. Biol. Chem.* **264**, 936-939. "Purification of a protein from bovine plasma that binds to type 1 plasminogen activator inhibitor and prevents its interaction extracellular matrix. Evidence that the protein is vitronectin."

Mimuro, J., Muramatsu, S., Kurano, Y., Uchida, Y., Ikadao, H., Watanabe, S., and Sakata, T. (1993) *Biochem.* **32** (9), 2314-20. "Identification of the plasminogen activator inhibitor-1 binding heptapeptide in vitronectin."

Morris, C. A., Underwood, P. A., Sheehan, M., and Charlesworth, J. A. (1994) *J. Biol. Chem.* **269** (38), 23845-23852. "Relative topography of biologically active domains of human vitronectin. Evidence from monoclonal antibody epitope and denaturation studies."

Mottonen, J., Strand, A., Symersky, J., Sweet, R. M., Danley, D. E., Geoghegan, K. F., Gerard, R. D., and Goldsmith, E. J. (1992) *Nature* **355**(6357), 270-3. "Structural basis of latency in plasminogen activator inhibitor-1"

Muller-Eberhard, H. J. (1986) *Ann. Rev. Immunol.* **4**, 503-508. "The membrane attack complex of complement."

Nar, H., Bauer, M., Stassen, J. M., Lang, D., Gils, A., and Declerck, P. J. (2000) *J Mol Biol* **297**(3), 683-95. "Plasminogen activator inhibitor 1. Structure of the native serpin, comparison to its other conformers and implications for serpin inactivation"

Ogawa, H., Yoneda, A., Seno, N., Hayashi, M., Ishizuka, I., Hase, S., and Matsumoto, I. (1995) *Eur J Biochem* **230**(3), 994-1000. "Structures of the N-linked oligosaccharides on human plasma vitronectin"

Ostermeier, C., Iwata, S., Ludwig, B., and Michel, H. (1995) *Nat. Struct. Biol.* **Oct**; **2**(10), 842-846. "Fv fragment-mediated crystallization of the membrane protein bacterial cytochrome c oxidase."



Owensby, D. A., Morton, P. A., Wun, T. C., and Schwartz, A. L. (1991) *J. Biol. Chem.* **266**(7), 4334-40. "Binding of plasminogen activator inhibitor type-1 to extracellular matrix of Hep G2 cells. Evidence that the binding protein is vitronectin."

Padmanabhan, J., and Sane, D. C. (1995) *Thromb Haemost* **73**(5), 829-34. "Localization of a vitronectin binding region of plasminogen activator inhibitor-1."

Panetti, T. S., and McKeown-Longo, P. J. (1993) *J Biol Chem* **268**(16), 11492-5. "The alpha v beta 5 integrin receptor regulates receptor-mediated endocytosis of vitronectin"

Panetti, T. S., Wilcox, S. A., Horzempa, C., and McKeown-Longo, P. J. (1995) *J Biol Chem* **270**(31), 18593-7. "Alpha v beta 5 integrin receptor-mediated endocytosis of vitronectin is protein kinase C-dependent"

Panetti, T. S., and McKeown-Longo, P. J. (1993) *J Biol Chem* **268**(16), 11988-93. "Receptor-mediated endocytosis of vitronectin is regulated by its conformational state"

Parker, C. J., Stone, O. L., White, V. F., and Bernshaw, N. J. (1989) *Br. J. Haematol.* **71**, 245-252. "Vitronectin (S-protein) is associated with platelets."

Patrick, M. L., Craven, R. S., and Woods, S. L. (eds) (1991) *Medical Surgical Nursing*. Edited by Crown, K., J.P. Lipincott, Philadelphia.

Peake, P. W., Greenstein, J. D., Pussell, B. A., Charlesworth, J. A., Moen, O., Fosse, E., Dregelid, E., Brockmeier, V., Anderson, C., Hog-assen, K., Venge, P., Mollnes, T. E., and Kierulf, P. (1996) *Clin. Exp. Immunol.* **106** (2), 416-422. "The behavior of human vitronectin in vivo: effects of complement activation, conformation and phosphorylation."

Peterson, C. B., and Blackburn, M. N. (1987) *J Biol Chem* **262**(16), 7559-66. "Antithrombin conformation and the catalytic role of heparin. II. Is the heparin-induced conformational change in antithrombin required for rapid inactivation of thrombin?"

Peterson, C. B., and Blackburn, M. B. (1998) *Submitted* "The size and stoichiometry of the vitronectin: PAI-1 complex. Unexpected features regarding their role in regulating plasmin activation."

Peterson, C. B. (1998) *Submitted* "Unexpected properties of Vitronectin:PAI-1 Complexes and their Role in Regulating Plasmin Activation."

Pierschbacher, M. D., and Ruoslahti, E. (1987) *J. Biol. Chem.* **262**, 17294-17298. "Influence of stereochemistry of the sequence Arg-Gly-Asp-Xaa on binding specificity in cell adhesion."



Ploug, M., Ronne, E., Behrendt, N., Jensen, A. L., Blasi, F., and Dano, K. (1991) *J Biol Chem* **266**(3), 1926-33. "Cellular receptor for urokinase plasminogen activator. Carboxyl-terminal processing and membrane anchoring by glycosyl- phosphatidylinositol"

Pokkuluri, P. R., Bouthillier, F., Li, Y., Kuderova, A., Lee, J. and Cygler, M. (1994). *J. Mol. Biol.* **243**, 283-297.

Podack, E. R., Kolb, W. P., and Muller-Eberhard, H. J. (1977) *J. Immunol.* **119**, 2024-2029. "The SC5b7-complex: formation isolation, properties, and subunit composition."

Podack, E. R., Kolb, W. P., and Muller-Eberhard, H. J. (1978) *J. Immunol.* **120**, 1841-1848. "The C5b6 complex: formation, isolation, and inhibition of its activity by lipoprotein and S-protein of human serum."

Podack, E. R., and Muller-Eberhard, H. J. (1979) *J. Biol. Chem.* **254**, 9908-9914. "Isolation of human S protein, an inhibitor of the membrane attack complex of complement."

Preissner, K. T., Wassmuth, R., Muller-Berghaus, G. (1985(a)) *Biochem. J.* **231**, 349-355. "Physiochemical characterization of human S-protein and its function in the blood coagulation system."

Preissner, K. T., Zwicker, L., Muller-Berghaus, G. (1985(b)) *Biochem. J.* **243**, 349-351. "Formation, characterization and detection of a ternary complex between S-protein, thrombin and antithrombin III."

Preissner, K. T., Zwicker, L., and Muller-Berghaus, G. (1987) *Biochem. J.* **243**(1), 105-111. "Formation, characterization and detection of a ternary complex between S protein, thrombin and antithrombin III in serum."

Preissner, K. T., and Muller-Berghaus, G. (1987) *J Biol Chem* **262**(25), 12247-53. "Neutralization and binding of heparin by S protein/vitronectin in the inhibition of factor Xa by antithrombin III. Involvement of an inducible heparin-binding domain of S protein/vitronectin"

Preissner, K. T., Holzhter, S., Justus, C., and Muller-Berghaus, G. (1989) *Blood* **74**, 1989-1996. "Identification and partial characterization of platelet vitronectin: Evidence for complex formation with platelet-derived plasminogen activator inhibitor-1."

Preissner, K. T. (1990) *Biochem. Biophys. Res. Commun.* **168**(3), 966-71. "Specific binding of plasminogen to vitronectin. Evidence for a modulatory role of vitronectin on fibrin(ogen)-induced plasmin formation by tissue plasminogen activator."

Preissner, K. T., Grulich-Henn, J., Ehrlich, H. J., Declerck, P., Justus, C., Collen, D., Pannekoek, H., and Muller-Berghaus, G. (1990) *J. Biol. Chem.* **265**, 18490-18498.



"Structural requirements for the extracellular interaction of plasminogen activator inhibitor-1 with endothelial cell matrix-associated vitronectin."

Preissner, K. T. (1991(a)) *Annu. Rev. Cell Biol.* 7, 275-310. "Structure and biological role of vitronectin."

Preissner, K. T. (1991(b)) *Thrombosis and Haemostasis* 66, 123-132. "Structure of vitronectin and its biological role in haemostasis."

Pytela, R., Pierschbacher, M.D., and Ruoslahti, E. (1985) *Proc. Natl. Acad. Sci.* 82, 5766-5770. "A 125/115KDa cell surface receptor specific for vitronectin interacts with the arginine-glycine-aspartic acid adhesion sequence derived from fibronectin."

Rousseaux, J., et al. (1983) *J. Immunol. Meth.* 64, 141-146. "Optimal conditions for the preparation of Fab and F(ab')<sub>2</sub> fragments from monoclonal IgG of different rat IgG subclasses."

Royle, G., Deng, G., Seiffert, D., and Loskutoff, D. J. (2001) *Anal Biochem* 296(2), 245-53. "A method for defining binding sites involved in protein-protein interactions: analysis of the binding of plasminogen activator inhibitor 1 to the somatomedin domain of vitronectin."

Rudd, P. M., Dwek, R. A. (1997) *Critical Reviews*, 32, 1-100. "Glycosylation: Heterogeneity and the 3D Structure of Proteins."

Ruoslahti, E., and Pierschbacher, M. D. (1987) *Science* 238, 491-497. "New perspectives in cell adhesion: RGD and integrins."

Sane, D. C., Moser, T. L., Parker, C. J., Seiffert, D., Loskutoff, D. J., and Greenberg, C. S. (1990) *J. Biol. Chem.* 265, 3543-3548. "Highly sulfated glycosaminoglycans augment the cross-linking of vitronectin by guinea pig liver transglutaminase. Functional studies of the cross-linked multimers."

Sane, D. C., Moser, T. L., and Greenberg, C. S. (1991) *Thromb. Haemost.* 66(3), 310-4. "Limited proteolysis of vitronectin by plasmin destroys heparin binding activity."

Sane, D. C., and Zhao, Y. (1993) in *Biology of Vitronectins and Their Receptors* (Preissner, K. T., Rosenblatt, S., Kost, C., Wegerhoff, J., and Mosher, D. F., eds), pp. 31-38., Elsevier, Amsterdam.

Seftor, R. E. B., Seftor, E. A., Stetlet-Stevenson, W. G., and Hendrix, M. J. C. (1993) *Cancer Res.* 53, 3411-3415. "The 72 kDa type IV collagenase is modulated via differential expression of alpha v beta 3 and alpha 5 beta 1 integrins during human melanoma cell invasion."



Seiffert, D., Keeton, M., Eguchi, Y., Saudey, M., Loskutoff, D. J. (1991(a)). Detection of vitronectin mRNA in tissues and cells of the mouses. *Proc. Natl. Acad. Sci.* **88**, 9402-9406.

Seiffert, D., and Loskutoff, D. J. (1991) *J Biol Chem* **266**(5), 2824-30. "Evidence that type 1 plasminogen activator inhibitor binds to the somatomedin B domain of vitronectin"

Seiffert, D., and Loskutoff, D. J. (1991). *Biochem. Biophys. Acta* **1078**, 23-30. "Kinetic analysis of the interaction between type one plasminogen activator inhibitor and vitronectin and evidence that the bovine inhibitor binds to a thrombin-derived amino-terminal fragment of bovine vitronectin."

Seiffert, D., and Loskutoff, D. J. (1991(b)). *J. Biol. Chem.* **266**, 2824-30. "Evidence that type 1 plasminogen activator inhibitor binds to the somatomedin B domain of vitronectin."

Seiffert, D., Crain, K., Wagner, N. V., and Loskutoff, D. J. (1994) *J. Biol. Chem.* **269** (31), 19836-42. "Vitronectin gene expression *in vivo*. Evidence for extrahepatic synthesis and acute phase regulation."

Seiffert, D., Ciambone, G., Wagner, N. V., Binder, B. R., and Loskutoff, D. J. (1994) *J Biol Chem* **269**(4), 2659-66. "The somatomedin B domain of vitronectin. Structural requirements for the binding and stabilization of active type 1 plasminogen activator inhibitor"

Seiffert, D., Moser, T. L., Enghild, J. J., Pizzo, S. V., and Stack, M. S. (1995) *FEBS Lett.* **368** (1), 155-159. "Evidence that conformational changes upon the transition of the native to the modified form of vitronectin are not limited to the heparin binding domain."

Seiffert, D. (1996). *J. Histochem. Cytochem.* **44** (3), 275-80. "Detection of vitronectin in mineralized bone matrix."

Seiffert, D., and Schleef, R. R. (1996) *Blood* **88**(2), 552-60. "Two functionally distinct pools of vitronectin (Vn) in the blood circulation: identification of a heparin-binding competent population of Vn within platelet alpha-granules."

Seiffert, D. (1996) *J. Biol. Chem.* **271**(19), 11170-11176. "Hydrolysis of platelet vitronectin by calpain."

Seiffert, D., and Smith, J. W. (1997) *J. Biol. Chem.* **272**(21), 13705-10. "The cell adhesion domain in plasma vitronectin is cryptic."

Seiffert, D. (1997) *J. Biol. Chem.* **272** (15), 9971-9978. "The glycosaminoglycan binding site governs ligand binding to the somatomedin B domain of vitronectin."



Sharp, A. M., Stein, P. E., Pannu, N. S., Carrell, R. W., Berkenpas, M. B., Ginsburg, D., Lawrence, D. A., and Read, R. J. (1999) *Structure Fold Des* **7**(2), 111-8. "The active conformation of plasminogen activator inhibitor 1, a target for drugs to control fibrinolysis and cell adhesion"

Shifman, M. A., and Pizzaro, S. V. (1982) *J. Biol. Chem.* **257**, 3243-3248. "The *in vivo* metabolism of antithrombin III complexes in blood."

Sigurdardottir, O., and Wiman, B. (1994) *Biochim Biophys Acta* **1208**(1), 104-10. "Identification of a PAI-1 binding site in vitronectin"

Sigurdardottir, O., and Wiman, B. (1994) *Biochim Biophys Acta* **1208**(1), 104-10. "Identification of a PAI-1 binding site in vitronectin"

Silverton, E. W., Padlan, E. A., Davies, D. R., Smith-Gill, S. & Potter, M. (1984). *J. Mol. Biol* **180**, 761-765.

Skorstengaard, K., Halkier, T., Hojrup, P., and Mosher, D. (1990). *FEBS Lett.* **262**, 269-274. "Sequence location of a putative transglutaminase cross-linking site in human vitronectin."

Smith, A., Tatum, F. M., Muster, P., Burch, M. K., and Morgan, T. (1988) *J. Biol. Chem.* **263**, 5224-5229. "Importance of Ligand-induced Conformational Changes in Hemopexin for Receptor-mediated Heme Transport."

Sobel, M., Soler, D. F., Kermode, J. C., and Harris, R. B. (1992) *J. Biol. Chem.* **267**, 8857-8862. "Localization and characterization of a heparin binding domain peptide of human von Willebrand factor."

Stanley, K. K. (1986) *FEBS Lett.* **199**, 249-253. "Homology with hemopexin suggests a possible scavenging function for S-protein/vitronectin."

Stockmann, A., Hess, S., Declerck, P., Timpl, R., and Preissner, K. T. (1993) *J. Biol. Chem.* **268**(30), 22874-82. "Multimeric vitronectin. Identification and characterization of conformation-dependent self-association of the adhesive protein."

Stura, E. A., Nemerow, G. R., and Wilson, I. A. (1992) *J Cryst Growth*, **122**, 273-285. "Strategies in the crystallization of glycoproteins and protein complexes."

Stura, E. A., Graille, M. J., and Charbonnier, J. -B. (2001a) *J. Cryst. Growth*, **232**, 573-579.

Stura, E. A., Graille, M. J., Sutton, B. J., Gore, M. G., Silverman, G. J., and Charbonnier, J.-B. (2001b) *J. Cryst. Growth*, **232**, 580-590.



Stura, E. A., Taussig, M. J., Sutton, B. J., Duquerroy, S., Bressanelli, S., Minson, A. C., and Rey, F. A. (2002) *Acta Cryst.* **D58**, 1715-1721. "Scaffolds for protein crystallization."

Suzuki, S., Pierschbacher, M. D., Hayman, E. G., Nguyen, K., Ohgren, Y., and Ruoslahti, E. (1984) *J Biol Chem* **259**(24), 15307-14. "Domain structure of vitronectin. Alignment of active sites"

Tschopp, J., Podack, E. R., and Muller-Eberhard, H. J. (1985). *J. Immunol.* **134**, 495-499. "The membrane attack complex of complement: C5b-8 as accelerator of C9 polymerization."

Tschopp, J., Masson, D., Schafer, S., Peitsch, M., and Preissner, K. T. (1988) *Biochemistry* **27**(11), 4103-9. "The heparin binding domain of S-protein/vitronectin binds to complement components C7, C8, and C9 and perforin from cytolytic T-cells and inhibits their lytic activities."

Thiagarajan, P., Le, A., Snuggs, M. B., and VanWinkle, B. (1996) *Cell Adhes. Commun.* **4**(4-5), 317-25. "The role of carboxy-terminalglycosaminoglycan-binding domain of vitronectin in cytoskeletal organization and migration of endothelial cells."

Thiagarajan, P., and Kelly, K. L. (1988) *J Biol Chem* **263**(6), 3035-8. "Exposure of binding sites for vitronectin on platelets following stimulation"

Tollefsen, D.M., Weigel, C.J., and Kabeer, M.H. (1990) *J. Biol. Chem.* **265**, 9778-9781. "The presence of methionine or threonine at position 381 in vitronectin is correlated with proteolytic cleavage at Arginine 379."

Tomasini, B. R., and Mosher, D. F. (1988) *Blood* **72**(3), 903-12. "Conformational states of vitronectin: preferential expression of an antigenic epitope when vitronectin is covalently and noncovalently complexed with thrombin-antithrombin III or treated with urea."

Tomasini, B. R., Owen, M. C., Fenton, J. W. d., and Mosher, D. F. (1989) *Biochemistry* **28**(19), 7617-23. "Conformational lability of vitronectin: induction of an antigenic change by alpha-thrombin-serpin complexes and by proteolytically modified thrombin."

Tomasini, B. R., and Mosher, D. F. (1991) in *Prog. In Hemostasis and Thrombosis* (Coller, B. S., ed) Vol. 10, pp. 269-305, W. B. Saunders Company.

Valentin-Weigand, P., Grulich-Henn, J., Chhatwal, G., Muller-Berghaus, G., Blobel, H., and Preissner, K. T. (1988) *Infect. Immunol.* **56**, 2851-2855. "Mediation of adherence of *streptococci* to human endothelial cells by complement S protein (vitronectin)."



van Meijer, M., Gebbink, R. K., Preissner, K. T., and Pannekoek, H. (1994) *FEBS Lett* **352**(3), 342-6. "Determination of the vitronectin binding site on plasminogen activator inhibitor 1 (PAI-1)."

Vassali, J. D., Vaccino, D., and Belin, D. (1985). *J. Cell Biol.* **100**, 86-92. "A cellular binding site for the Mr 55,000 form of the human plasminogen activator, urokinase."

Volker, W., Hess, S., Vischer, P., and Preissner, K. T. (1993) *J. Histochem. Cytochem.* **41** (12), 1823-1832. "Binding and processing of multimeric vitronectin by vascular endothelial cells."

Wachenberg, B. L., Liberman, B., Gomes, E., and Pierone, R. R. (1980) *Horm. Metab. Res.* **12**, 516-519. "Radioimmunoassayable serum somatomedin B in normal subjects and in patients with acromegaly and pituitary dwarfism: effects of human growth hormone therapy."

Wadstrom, T., Ljungh, A., and Flock, J. I. (1993) in *Biology of Vitronectins and Their Receptors* (Preissner, K. T., Rosenblatt, S., Kost, C., Wegerhoff, J., and Mosher, D. F., eds), Elsevier, Amsterdam.

Wallon, U. M., and Overall, C. M. (1997) *J. Biol. Chem.* **272**, 7473-7481. "The hemopexin-like domain (C domain) of human gelatinase A (matrix metalloproteinase-2) requires  $\text{Ca}^{2+}$  for fibronectin and heparin binding."

Waltz, D. A., and Chapman, H. A. (1994). *J. Biol. Chem.* **269** (20), 14746-14750. "Reversible cellular adhesion to vitronectin linked to urokinase receptor occupancy."

Waltz, D. A., Natkin, L. R., Fujita, R. M., Wei, Y., and Chapman, H. A. (1997) *J Clin Invest* **100**(1), 58-67. "Plasmin and plasminogen activator inhibitor type 1 promote cellular motility by regulating the interaction between the urokinase receptor and vitronectin"

Weber, P. C. (1991) *Adv. Prot. Chem.* **41**:1-36. "Physical principles of protein crystallization."

Wei, Y., Waltz, D. A., Rao, N., Drummond, R. J., Rosenberg, S., and Chapman, H. A. (1994). *J. Biol. Chem.* **269** (51), 32380-32388. "Identification of the urokinase receptor as an adhesion receptor for vitronectin."

Wiman, B., Almquist, A., Sigurdottir, O., and Lindahl, T. (1988). Plasminogen activator inhibitor (PAI-1) is bound to vitronectin in plasma. *FEBS Lett.* **242**, 125-128.

Wind, T., Jensen, M. A., and Andreasen, P. A. (2001) *Eur J Biochem* **268**(4), 1095-1106. "Epitope mapping for four monoclonal antibodies against human plasminogen activator



inhibitor type-1 Implications for antibody-mediated PAI-1-neutralization and vitronectin-binding."

Xu, Y., Xu, D., and Uberbacher, E. C. (1998) *J. Comp. Biol.* **5**, 597-614. "An efficient computational method for globally optimal threading."

Xu, D., Baburaj, K., Peterson, C. B., and Xu, Y. (2001) *Proteins* **44**(3), 312-20. "Model for the three-dimensional structure of vitronectin: Predictions for the multi-domain protein from threading and docking."

Yoneda, A., Ogawa, H., Kojima, K., and Matsumoto, I. (1998) *Biochemistry* **37**(18), 6351-60. "Characterization of the ligand binding activities of vitronectin: interaction of vitronectin with lipids and identification of the binding domains for various ligands using recombinant domains"

Zheng, X., Saunders, T. L., Camper, S. A., Samuelson, L. C., and Ginsburg, D. (1995) *Proc Natl Acad Sci U S A* **92**(26), 12426-30. "Vitronectin is not essential for normal mammalian development and fertility"

Zhou, G. W., Guo, J., Huang, W., Fletterick, R. J. and Scanlan, T. S. (1994) *Science*, **265**, 1059-1064.

Zhuang, P., Li, H., Williams, J. G., Wagner, N. V., Seiffert, D., and Peterson, C. B. (1996) *J Biol Chem* **271**(24), 14333-43. "Characterization of the denaturation and renaturation of human plasma vitronectin. II. Investigation into the mechanism of formation of multimers"

Zhuang, P., Chen, A. I., and Peterson, C. B. (1997) *J Biol Chem* **272**(11), 6858-67. "Native and multimeric vitronectin exhibit similar affinity for heparin. Differences in heparin binding properties induced upon denaturation are due to self-association into a multivalent form"

Zhuang, P., Blackburn, M. N., and Peterson, C. B. (1996) *J. Biol. Chem.* **271**, 14323-14332. "Characterization of the Denaturation and Renaturation of Human Plasma Vitronectin. I. Biophysical Characterization of Protein Unfolding and Multimerization."

Zhou, Y. and MacKinnon, R. (2001) *NSLS Activity Report*. "Fab-mediated Crystallization of a Potassium Channel." Howard Hughes Medical Institute, Laboratory of Molecular Neurobiology and Biophysics, Rockefeller University, New York, NY



